Ophicalcites from the northern Pyrenean belt: a field, petrographic and stable isotope study

Camille Clerc, Philippe Boulvais, Yves Lagabrielle, Michel de Saint Blanquat

Ophicalcites from the Northern Pyrenean Belt: a field, petrographic and stable isotope study.

by:

Camille Clerc (1), Boulvais Philippe (2), Yves Lagabrielle (3) and Michel de Saint Blanquat (4)

(1) Laboratoire de Géologie, CNRS-UMR 8538, Ecole Normale Superieure, 24 rue Lhomond, 75231 Paris Cedex 5, France.

(2) Géosciences Rennes, CNRS-UMR 6118, Université de Rennes 1, Campus de Beaulieu, 35042, Rennes Cedex, France

(3) Géosciences Montpellier, CNRS-UMR 5243, Université de Montpellier 2, Place Eugène Bataillon, 34095 Montpellier, France

(4) GET, CNRS-UMR 5563, Université Paul Sabatier, 14 avenue Edouard Belin, 31400 Toulouse, France.

Corresponding author:

Camille Clerc

clerc@geologie.ens.fr

Abstract

Brecciated and fractured peridotites with a carbonate matrix, referred to as *ophicalcites,* are common features of mantle rocks exhumed in passive margins and mid-oceanic ridges. Ophicalcites have been found in close association with massive peridotites, which form the numerous ultramafic bodies scattered along the North Pyrenean Zone (NPZ), on the northern flank of the Pyrenean belt. We present the first field, textural and stable isotope characterization of these rocks. Our observations show that Pyrenean ophicalcites belong to three main types: (1) a wide variety of breccias composed of sorted or unsorted millimeter-to meter-sized clasts of fresh or oxidized ultramafic material, in a fine-grained calcitic matrix; (2) calcitic veins penetrating into fractured serpentine and fresh peridotite; and (3) pervasive substitution of serpentine minerals by calcite. Stable isotope analyses (O, C) have been conducted on the carbonate matrix, veins and clasts of samples from 12 Pyrenean ultramafic bodies. We show that the Pyrenean ophicalcites are the product of three distinct genetic processes: i) pervasive ophicalcite resulting from relatively deep and hot hydrothermal activity; ii) ophicalcites in veins resulting from tectonic fracturing and cooler hydrothermal activity; and iii) polymictic breccias resulting from sedimentary processes occurring after the exposure of subcontinental mantle as portions of the floor of basins which opened during the mid-Cretaceous. We highlight a major difference between the Eastern and Western Pyrenean ophicalcites belonging respectively to the sedimentary and to the hydrothermal types. Our data set points to a possible origin of the sedimentary ophicalcites in continental endorheic basins, but a post-depositional evolution by circulation of metamorphic fluids or an origin from relatively warm marine waters cannot be ruled out. Finally, we discuss the significance of such discrepancy in the characterics of the NPZ ophicalcites in the frame of the variable exhumation history of the peridotites all along the Pyrenean realm.

Key words: ophicalcite, ophicarbonate, stable isotopes, oxygen, carbon, veins, matrices, Pyrenees, Lherz, Urdach, mantle exhumation, tectonic fracturation, hydrothermalism, sedimentary deposits.

I. Introduction

During uplift and exhumation of the sub-continental mantle, the peridotites are commonly serpentinized through interactions with fluids, with direct consequences on their bulk density and their rheological, seismic, gravimetric and magnetic properties (Brun & Beslier 1996; Boschi et al. 2006). In oceanic and passive margin environments, besides serpentinization, the peridotites show evidence of carbonation expressed through the occurrence of a bimodal, ultramafic and carbonate association known as ophicalcites or ophicarbonates (Spooner & Fyfe 1973; Bonatti et al. 1974; Dietrich et al. 1974; Gianelli & Principi 1977; Ohnenstetter 1979; Lemoine 1980; Cortesogno et al. 1981; Lagabrielle & Cannat 1990). More recently, the carbonation of the exhumed mantle rocks has been clearly described as the last event affecting faulted rocks uprising along oceanic detachment faults at the axis of slow-spreading ridges (Picazo et al. 2012).

Ophicalcites were first discovered in the Ligurian Alps (Bonney 1879), and then described in many ophiolite sequences (see Artemyev & Zaykov 2010 and Bogoch 1987 for a comprehensive historical literature on ophicalcites). Ophicalcites commonly display large variations in the proportions of ultramafic and carbonate material. They range from in-situ fractured peridotites with carbonate infill, through clast-supported breccias with multiple generations of carbonate infilling and internal sediments, to matrix-supported breccias. Lemoine et al. (1987) distinguish two main types of ophicalcite. Ophicalcite type 1 (OC1) is represented by massive serpentinites exhibiting a dense mesh of calcite-infilled fractures. Ophicalcite type 2 (OC2) refers to sedimentary breccias having a calcitic matrix, often deposited above ophicalcite of type 1. The clasts comprise sorted or unsorted millimeter- to meter-sized fresh or oxidized ultramafic fragments. In some cases, exotic clasts of gabbroic or basaltic composition can be observed. The matrix of OC2 is either a fine-grained calcitic

sediment or a cement consisting of sparry calcite. It varies in color from red to pink and gray to green, depending on the chlorite or hematite content; sparry calcite is generally white. Ophicalcites often record a polyphase history, revealed by different generations of cements and sediment infill, which can be highlighted by color changes, and bimodal grain distribution (Abbate et al. 1970; Bonatti et al. 1974; Bernoulli & Weissert 1985; Lemoine et al. 1987; Früh-Green et al. 1990).

Because of the wide variety of ophicalcites and their occurrence in different oceanic or continental margin settings, it is important to recall that the term ophicalcite does not refer to a genetic process, but to a generic rock-type. Among the processes invoked for their formation one group refers to endogenic evolution, involving various deep seated phenomena such as: (1) mantle originated gas seeps (Bonatti et al. 1974; Haggerty 1991; Kelemen et al. 2004); (2) magmatic intrusions (Cornelius 1912; Bailey & McCallien 1960); (3) contact and regional metamorphism (Peters 1965; Trommsdorff et al. 1980) and (4) hydrothermal fluid interactions (Cornelius 1912; Lavoie & Cousineau 1995; Artemyev & Zaykov 2010). Another group refers to surficial processes involving mechanical mixing of carbonates and ultramafic rocks through tectonic crushing, sedimentary reworking and gravity-driven infilling of veins and fractures (Bortolotti & Passerini 1970; Knipper 1978; Bernoulli & Weissert 1985; Früh-Green et al. 1990; Treves & Harper 1994; Treves et al. 1995; Knipper & Sharas'kin 1998).

In the French Pyrenees, ophicalcites have been reported in some ultramafic bodies associated with mid-Cretaceous basins and recently re-interpreted as resulting from mantle exhumation during Mid-Cretaceous rifting (Lagabrielle & Bodinier 2008; Lagabrielle et al. 2010; Jammes et al. 2009; Clerc et al. 2012). In order to document and to characterize the variable typology of ophicalcites and to decipher their origin with respect to exhumation processes, we have performed a comprehensive field, petrological and geochemical study of samples taken throughout the Pyrenees (fig. 1). We identify three types of ophicalcites related to three

distinct genetic processes: i) pervasive ophicalcite resulting from replacement of ultramafic minerals due to relatively deep and hot hydrothermal activity, ii) ophicalcites as veins resulting from tectonic fracturing and cooler hydrothermal activity and iii) polymictic breccias resulting from syn-sedimentary processes. The first two types record the activity associated with the final emplacement of the peridotites, whereas the last one is associated with the final exhumation of mantle rocks as portions of the basement of newly formed basins.

II. Geological setting of the ultramafic Pyrenean bodies:

The Pyrenees are a narrow, 400 km long continental fold and thrust belt resulting from the collision of the northern edge of the Iberian Plate and the southern edge of the European Plate during the late Cretaceous to Tertiary (Choukroune & ECORS Team 1989; Muñoz 1992; Deramond et al. 1993; Roure & Combes 1998; Teixell 1998). Triassic and Jurassic aborted rifting events predated the development of a major Cretaceous crustal thinning event, which culminated in displacement between the Iberian and European plates (Puigdefàbregas & P. Souquet 1986; Vergés & Garcia-Senz 2001). Continental rifting in the Pyrenean domain occurred in response to the counterclockwise rotation of Iberia relative to Europe, coeval with the onset of oceanic spreading in the Bay of Biscay between Chron M0 and A33o (approximately 125-83 Ma) (Le Pichon et al. 1970; Choukroune & Mattauer 1978; Olivet 1996; Gong et al. 2008; Jammes et al. 2009). About forty metric- to kilometric-sized fragments of subcontinental mantle rocks are found along the northern flank of the Pyrenees, in the North Pyrenean Zone (NPZ). They reside within or next to numerous lozenge-shaped basins flanking the North Pyrenean Fault (NPF). These basins are interpreted as the remnants of isolated, pull-apart or transtensive half graben basins formed in response to the eastward drift of Iberia along the NPF and later inverted during the Late Cretaceous-Early Cenozoic

Pyrenean orogeny (Le Pichon et al. 1970; Choukroune & Mattauer 1978). A typical flysch sedimentation started during the mid-Albian within these basins (black flysch), which later enlarged during the Late Albian and connected into one single, wider basin trough during the Cenomanian (Debroas 1976; P. Souquet et al. 1985; Debroas 1990).

Various scenarios have been proposed for the emplacement of the ultramafic bodies, ranging from purely tectonic mechanisms, such as solid intrusion of hot or cold mantle rocks into sediments during strike-slip events (Avé-Lallemand 1967; Minnigh et al. 1980; Vielzeuf & Kornprobst 1984), to tectono-sedimentary processes in which mantle rocks were exhumed during Variscan time (Mattauer & Choukroune 1974; Fortane et al. 1986) and reworked in a mid-Cretaceous wild flysch (Fortane et al. 1986). In recent re-examinations, various authors propose that some of these bodies are fragments of sub-continental mantle basement partially exhumed during Albian-Cenomanian times (Lagabrielle & Bodinier, 2008; Jammes et al. 2009; Lagabrielle et al. 2010; Debroas et al. 2010; Clerc et al. 2012). Within the NPZ, the metasediments are locally strongly deformed and underwent a High Temperature - Low Pressure (HT-LP) mid-Cretaceous metamorphic event, which lasted nearly 30 Ma from 110 Ma to 80 Ma (Azambre & Rossy 1976; Albarède & Michard-Vitrac 1978b; Montigny et al. 1986; Golberg et al. 1986; Goldberg & Maluski 1988; Thiébaut et al. 1988; Thiébaut et al. 1992). This metamorphism is considered as a consequence of crustal thinning (Golberg & Leyreloup 1990) and developed in relation with hydrothermal circulations (Dauteuil & Ricou 1989). Hydrothermal circulations are also responsible for extensive albitization of some of the North Pyrenean Massifs (Demange et al. 1999; Boulvais et al. 2007; Poujol et al. 2010), and formation of massive talc deposits (Moine et al. 1989; Schärer et al. 1999; Boulvais et al. 2006) probably in relation to the activity of major ductile extensive shear-zones (Passchier 1984; St Blanquat et al. 1986; Costa & Maluski 1988; St Blanquat et al. 1990; St Blanquat 1993).

III. Geology of the sampling sites

The ophicalcites and related ultramafic breccias selected for the oxygen and carbon isotope study were sampled from peridotite bodies exposed all along the NPZ (fig. 1). We selected nine localities which are representative of the variety of the Pyrenean peridotites, and presumably of the different geological processes involved in their exhumation history. Two sampling sites are located in the western Pyrenees (Urdach and Tos de la Coustette), one in the central Pyrenees (Moncaup) and nine in the Eastern Pyrenees (Ercé-Angladure, Lherz, Fontête Rouge, Freychinède, Berqué, Vicdessos, Urs, Bestiac, Caussou).

III.1. Western peridotites

Several peridotite bodies outcrop in the Chaînons Béarnais, within the fold and thrust belt Mesozoic sequence of the NPZ, at a longitude corresponding to the western termination of the Paleozoic Pyrenean axial zone. The base of the stratigraphic sequence, exposed along the Mail Arrouy, Sarrance and Layens post-Cenomanian thrusts (Casteras 1970), is composed of Late Triassic evaporites, breccias and ophites overlain by Mesozoic platform carbonates forming the original cover of the northern Iberian margin (Canérot et al. 1978; Canérot & Delavaux 1986). In contrast to the Eastern NPZ, evidence of HT-LP metamorphism is restricted here to some scarce and narrow regions bordering fault contacts with Triassic and mantle rocks (Fortane et al. 1986; Thiébaut et al. 1992; Lagabrielle et al. 2010) and the temperatures during peak metamorphism barely exceeded 400°C (Clerc 2012). Petrological and geothermobarometric studies of the western ultramafic bodies show that they underwent a two step exhumation with a first rise from 60 km to 25 km depth (1050-950°C), probably during late Hercynian times, followed by a further step from 25 km to a shallower and cooler

(600°C) level (Fabriès et al., 1998). This second step is marked by the development of a mylonitic fabric, from 117 Ma to 109 Ma (Vissers et al. 1997; Fabriès et al. 1998).

The Urdach body is a 1.5 km wide peridotite slice exposed at the western termination of the Mail Arrouy thrust (fig. 2A). It is overlain by Paleozoic basement slices and surrounded on its western and southern sides by a large volume of unsorted sedimentary breccias and olistoliths composed of peridotite fragments associated with Paleozoic basement clasts from upper, middle and lower crustal levels. These debris are intermingled in the Cenomanian black flysch (Casteras 1970; Vielzeuf 1984; Souquet et al. 1985; Jammes et al. 2009; Debroas et al. 2010). Some authors considered that the Urdach body itself might be an olistolith settled in Cenomanian sediments (Duée et al. 1984; Fortane et al. 1986). Peridotite hydrothermal alteration led to pervasive serpentinization reaching 80%. This is a dominant character of the Urdach body (Fabriès et al. 1998).

The 400 m long Tos de la Coustette ultramafic body is located 3 km west of the Saraillé summit, at the western termination of the Sarrance anticline (fig 2a). Apart from the peridotites, the faulted heart of the Sarrance anticline includes, Paleozoic basement rocks and ophite lenses embedded within cataclastic Triassic sediments. It is thrusted over the verticalized Urgonian limestones and Albian flysch of the Lourdios Syncline (Casteras 1970; Lagabrielle et al., 2010). The Tos de la Coustette body itself is in tectonic contact with small lenses of Paleozoic crustal rocks and Triassic metaevaporites outcropping both above and beneath the peridotites. Like the Saraillé peridotites, the environment of the Tos de la Coustette body is devoid of sedimentary breccias; instead these bodies are entirely surrounded by cataclastic breccias limited by tectonic contacts and are thought never to have been exposed to the seafloor (Canérot & Delavaux 1986; Lagabrielle et al. 2010).

III.2. Central peridotites

The Moncaup ultramafic body is part of a group of peridotites exposures lying around the Milhas massif, in the central Pyrenees (fig. 1). They are associated with basement rocks, variably brecciated Triassic sediments, ophites and Albian mafic intrusions. They are overlain in tectonic contact by highly metamorphosed Mesozoic marbles (Debeaux & Thiébaut 1958; Hervouët et al. 1987; Barrère et al. 1984). Although the peridotites have risen to near surface levels, there is no evidence for sedimentary reworking indicating their exhumation on the basin floor. Indeed, based on their geological setting, it can be deduced that the mantle rocks have remained capped by the Mesozoic marbles together with small slices of continental crust, during their uplift along the detachment fault (Lagabrielle et al. 2010).

III.3. Eastern peridotites:

The eastern Pyrenean peridotites are found within narrow belts of Mesozoic sediments of the NPZ, mainly limestones, pinched between the Axial Zone to the south and blocks of Paleozoic crust to the North representing the continental basement of the NPZ (North Pyrenean massifs) (fig. 1). Although the eastern Pyrenean mantle outcrops are often small and disconnected from an original substratum, one can still observe, on a decametric scale, a progressive transition from carbonate-free massive peridotites to high carbonate content breccias with all intermediates. On the rim of the ultramafic bodies, the massive peridotites are often crosscut by millimetric to centimetric calcite veins over the first few meters. In addition, in many localities, the peridotites are reworked within sedimentary polymictic breccias together with highly variable proportions of carbonate clasts. The amount of matrix of these breccias increases toward the carbonated end-member.

223 Most of the ultramafic bodies sampled for this study, from West to East, namely Ercé-
224 Angladure, Lherz, Fontête Rouge, Freychinède, Berqué, Vicdessos, Urs, Bestiac and Caussou,
225 display geological settings consistent with an origin as olistoliths surrounded by polymictic
226 detritic formation (fig. 2B, 3). They are interpreted as sedimentary records of the exhumation
227 of the peridotites on the floor of the Cretaceous basins (Lagabrielle & Bodinier 2008; Clerc et
228 al. 2012). The ultramafic-bearing breccias show sedimentary features such as grain-sorting
229 and crossbeddings and can be found away from the main bodies, indicating that they have
230 been transported by sedimentary processes. Lagabrielle & Bodinier (2008) showed that the
231 polymictic ultramafic-carbonate clastic sediments have been emplaced into fissures opened
232 within the exhumed massive peridotites, in a way similar to OC2 sedimentary ophicalcites of
233 Lemoine et al. (1987). Similar features are reported in more detail, together with the presence
234 of ultramafic-rich debris flows and evidence of ultramafic rock-fall in the vicinity of the
235 Lherz body by Clerc et al. (2012). The peridotites show little serpentinization, developed
236 mainly along discrete, localized joints and fissures. The carbonates reworked in the detritic
237 formations surrounding the peridotites are strongly deformed and underwent HT-LP
238 metamorphism with peak temperatures commonly as high as 600°C (Golberg & Leyreloup,
239 1990; Clerc 2012). By contrast to the western peridotites, the eastern ones underwent a single
240 and rapid uplift event, which probably limited hydrothermal alteration and serpentinization
241 (Albarède & Michard-Vitrac 1978a; Fabriès et al. 1991; Henry et al. 1998).

242

243 IV. Description of the analyzed samples

244 IV.1. Sampling strategy and collected samples

245 The sampling strategy was to collect samples from the four main geological environments
246 identified and distinguished as follows: (1) poorly serpentinized peridotites surrounded by hot

metasediments (Eastern and central peridotites) either exhumed to the basin floor (Lherz, Bestiac, Caussou, Vicdessos, Urs, Ercé-Angladure) or only unroofed but never exhumed (Moncaup), and (2) highly serpentinized peridotites surrounded by cooler sediments (Western peridotites) either exhumed to the basin floor (Urdach) or only unroofed but never exhumed (Tos de la Coustette). The list of the 48 studied samples is given in Table 1. We focused this study on the Lherz and Urdach bodies since they are among the largest mantle outcrops in the Pyrenees and because they represent two well-studied end-members in terms of their geological environment. Furthermore, these two localities offer better outcrop conditions compared with the smaller bodies poorly exposed in areas presenting important vegetal covering and rock alteration.

IV.2. Field and macroscopic aspects:

IV.2.a. Western Pyrenean Ophicalcites:

The western ophicalcites appear essentially as veins of calcite infilling fissures and fractures opened within the ultramafic rocks. The fractures present relatively constant and repeated orientations (fig. 4A). Particularly well observable in a quarry opened on the western side of the Urdach lherzolite body, they were first described by Monchoux (1970) and later interpreted as typical ophicalcite textures by Jammes et al. (2009). These authors highlighted their similarities with structures observed within exhumed mantle in the Alps and drilled off Iberia (Manatschal 2004). They consist mainly in millimetric to decimetric veins of clear white calcite (fig. 4B). The thickest veins are actually constituted of an accumulation of numerous veins and veinlets separated by thin fragments of peridotite strapped from the rims.

At Tos de la Coustette, the ophicalcites also appear as a dense mesh of very fine veinlets and as a pervasive substitution of serpentine minerals by patches of carbonate, barely visible on a

macroscopic scale, invading highly serpentinized peridotites (fig. 4C and D). Similar textures have also been described further east in the Avezac-Moncaut peridotites (Fabriès et al. 1998).

IV.2.b. Central Pyrenean Ophicalcites:

At least two types of ophicalcites were identified in the Moncaup peridotites. The first one, observed close to the damage zone of the tectonic contact between the peridotites and the overlying marbles, is represented by millimetric veins of coarse translucent sparite (fig. 4E). The veins crosscut and hence post-date a mylonitic fabric affecting the peridotites. The second one, observed in the damage zone of the detachment fault, consists of light brown micro-conglomerates and micrite infilling veins and cavities opened in the altered and dislocated peridotites (fig. 4F). The cavities present contorted and rounded rims. The micro-sediments show complex multi-generation evolutions with successive stages of deposition indicated by several color shades and crosscutting sparitic veins. The micro-conglomerates are laminated and present clear grain-sorting.

IV.2.c. Eastern Pyrenean Ophicalcites:

In the Eastern Pyrenees, ophicalcites and polymictic ultramafic-marble bearing breccias are observed within, close to, and even far away from the main peridotite bodies. Most of the clasts are composed either of ultra-fresh subcontinental peridotites or of marbles bearing mineral assemblages typical of the HT-LP mid-Cretaceous metamorphism. They are associated with a minor proportion of fragments deriving from gabbros, Triassic ophites Mesozoic meta-pelites and meta-evaporites and Paleozoic basement rocks (Lagabrielle & Bodinier 2008; Clerc et al. 2012).

In the Etang de Lherz area, Lagabrielle and Bodinier (1998) identified four main types of breccias and ophicalcites that can be extended to the other peridotite outcrops of the Eastern Pyrenees. (i) Type 1 is found in direct contact with or within the ultramafic body, it consists

294 of a carapace of monomictic breccias resulting from the cataclastic deformation of the
295 peridotites during exhumation. These breccias typically lack carbonate clasts and contain little
296 to no carbonate veins and cement. Therefore, they will not be considered further in this study.
297 (ii) Type 2 breccias, generally found in close contact with type 1 breccias, are ultramafic-
298 dominated polymictic breccias resulting from the sedimentary reworking of type 1. (iii) Type
299 3 breccias consist of thin layers of graded ultramafic litharenites bearing isolated cm-sized
300 clasts of peridotites and marbles and presenting slumps and syn-sedimentary normal faults
301 (fig. 5A and B). Within the type 3 breccias, the peridotite clasts display many different
302 lithologies (lherzolite, harzburgite, websterite, pyroxenite etc.), variable mantle textures
303 (equant coarse-granular to mylonitic) and variable degrees of serpentinization (totally fresh to
304 fully serpentinized, fig. 5C and D). These observations point to mixing and transport from a
305 relatively distant source by sedimentary processes. Furthermore, clasts of former monomictic
306 carbonate breccias and polymictic UM-marble breccia are also reworked in these formations,
307 pointing to their late deposition with regard to the exhumation history (Clerc et al., 2012). (iv)
308 Type 4 breccias correspond to clastic rocks closely resembling the OC2 sedimentary
309 ophicalcites of Lemoine et al. (1987). Clear white calcite veins penetrate fractured ultramafic
310 blocks in which they separate angular fragments. There is a striking association of these veins
311 with matrix-supported microbreccias similar to those forming the matrix of the type 2 breccias
312 (fig. 5E). The veins are smoothly rooted in the matrix and seem to be its extension in narrow
313 domains where the clasts were too big to fit. However, some veins crosscut pre-existing
314 matrices, pointing to a contemporaneous formation of matrices and veins during
315 sedimentation accompanied by multi-stage circulations of cementing fluids. In some outcrops,
316 the ultramafic clasts exhibit a centimeter thick orange-brown oxidation ring on their contact
317 with carbonate matrices and veins (fig. 5 E and F). This feature is also commonly observed in
318 oceanic ophicalcites (Boschi et al. 2006; Dick et al. 2008). This oxidation pattern does not

appear on the rims of the thinnest veins.

Ophicalcites at the Bestiac locality show similar features and offer exceptional conditions to investigate the successive generations of serpentinization and carbonation. The peridotite consists of tens of lens-shaped bodies less than a few hundred meters in size and embedded in a metamorphic bimodal ultramafic-marble breccia. Angular to slightly rounded centimeter-sized clasts of lherzolite are found more than 500 m away from the main blocks, a pattern clearly not consistent with any fault-assisted mode of emplacement. A few outstanding outcrops are visible in several abandoned caves and galleries dug for prospection of asbestos. Fresh to dark green serpentinites are crosscut by networks of cm-thick light green fibrous serpentine (likely chrysotile) delimitating metric lumps which mimict at a meter-scale the classical microscopic mesh-texture of serpentinized peridotites (Wicks & Whittaker 1977) (fig. 5G). The serpentine veins commonly show oblique sigmoidal fibers indicating shearing contemporaneous to brittle deformation responsible for vein development. Pluri-millimetric veins of calcite crosscut through this latest generation of serpentine veins that acted as a weak gateway for sediments and fluids during the ultimate stage of deformation and sedimentary reworking (fig. 5H). Some of the calcitic veins have a reddish coloration and increased concentration of oxides, suggesting possible syn- or post-diagenetic hydrothermal circulation. As in the Lherz area, these remarkable ultramafic-bearing formations have a relatively restricted extension and appear within large volumes of clastic formations devoid of any ultramafic component.

IV.3. Microscopic description:

Ophicalcite from the Urdach ultramafic body have millimetric veins of sparite. Several vein generations crosscut each other with varying angles. The calcite veins commonly show crack-

seal aspects. Symmetric layers of calcite with varying intensity in transmitted light and cathodoluminescence (CL), induced by minor variations of composition or inclusion concentration, are separated by a central suture (fig. 6A). Some of the largest veins actually consist of an accumulation of numerous sub-parallel veinlets, less than a micrometer wide, invading the serpentinite (fig. 6B). Finally, some other veins show zonated botryoids of fibrous radiating calcite (fig. 6C)

In the Tos de la Coustette ophicalcites, the carbonates mainly appear as micrometric to millimetric patches of calcite extensively dispersed within the serpentinite (fig. 6D). Intimate repartition of calcite and serpentine indicate a pervasive calcification by replacement of some serpentinous phases. The poorly elongated calcite aggregates develop following a general foliation marked by magnetite alignments and thin yellow serpentine veinlets. Surface estimate by digital image treatment indicates that the rock includes up to 55 % calcite, 40 % serpentine and 5 % magnetite with minor phases.

The matrix of the eastern Pyrenean ophicalcites and associated polymictic breccias consists of a pale-orange litharenite composed of infra-millimeter-sized angular clasts of marbles mixed with varyingly serpentinized ultramafic clasts and isolated minerals (pyroxenes, olivine, green and brown spinels). This litharenite sometimes appears laminated and shows graded-bedding due to sedimentary transport (Lagabrielle & Bodinier 2008; Clerc et al. 2012) (fig. 6E). In contrast to the veins, the matrices of the breccias, show much less evidence for recrystallization: there are, for example, a few newly formed metamorphic phyllosilicates and amphiboles.

Most of the veins observed in the Eastern Pyrenean ophicalcites consist of clear and equant sparry calcites (fig. 6F). The veins cross cut alternatively the ultramafic clasts and the matrix of the breccias in which they often seem to be rooted. In the simplest cases, a single

generation of calcite crystal nucleates from the rims of the veins and grows toward the center where it joins in a central suture. In some cases, the growth resumed or the fracture was reopened, leading to the formation of vugs. Most of the veins show multistep histories with successive infillings of sparite particularly well highlighted by varying luminescence in CL (fig. 6G). When pure enough, the veins are clearly recrystallized as evidenced by the conservation of former zoned calcite dogteeth ghosts within bigger equant neoformed crystals. The borders of the neoformed crystals are independent from those of the ghosts that they overprint (fig. 6H). When thick enough, the veins are generally filled with detrital material including micro-fragments of serpentine, oxides and calcite clasts mixed within a micrite. Although they lack microfossils, such veins resemble the neptunian dykes and veins formed on the subaquatic floor and consequently opened to sedimentary influx (Smart et al. 1987; Laznicka 1988; Winterer et al. 1991).

V. Methods for determination of O and C isotope compositions

Rock samples were sawed to select well-oriented and relevant planes. The sawed faces were cleaned using water and pulsed with dry air before micro-drilling. A minimum of about 20 mg of powder was collected for each sampling site.

The O and C isotope compositions were measured using a VG SIRA 10 triple collector mass spectrometer at the University of Rennes 1, on the CO_2 released during reaction of calcite with anhydrous H_3PO_4 in sealed vessels at 50°C (McCrea 1950). NBS 19 and internal-lab standard references materials (Prolabo Rennes) were continuously measured during the course of this work. NBS 19 measured values were $\delta^{18}O$ = 28.26 ± 0.09 (1σ, n=12) ‰ and $\delta^{13}C$ = 1.86 ± 0.02 (1σ, n=12) ‰. Results were corrected in accordance with the NBS 19 recommended values of 28.65‰ and 1.95‰, for O and C respectively. The analytical uncertainty is estimated at 0.15‰ and 0.1‰ for O and C.

VI. Results

The isotope compositions for the 48 analyzed samples are presented in table 1 and figure 7. The calcite phase found in clasts, veins and matrices from the Pyrenean ophicalcites and ultramafic-bearing breccias displays a wide range of oxygen isotope compositions with minimum values of 12.6 and 13.8‰ (vs. SMOW) measured in Moncaup and Tos de la Coustette veins (Western ophicalcites), and maximum values of 25.1‰ in the matrices of samples from Etang de Lherz area (fig. 4 & 6; Eastern ophicalcites). The carbon isotope compositions range from -5.8‰ (vs. PDB) in Moncaup samples to 1.5‰ in Lherz samples (matrices). As a whole, the field of isotopic compositions of Pyrenean ophicalcites is displaced from the one of the Iberian margin ophicalcites by lower $\delta^{18}O$ values and slightly lower $\delta^{13}C$ values (arrow in figure 7). Whereas no clear distinction can be made when comparing Pyrenean ophicalcites with Alpine and Apenninic ones, it seems that hydrothermal ophicalcite worldwide compare well with ophicalcites from the Western Pyrenees. First order analysis of the distribution of the oxygen and carbon isotope compositions implies to distinguish two separate domains: i) Ophicalcites from the Urdach and Tos de la Coustette ultramafic bodies have rather low and variable values of $\delta^{18}O$ and $\delta^{13}C$, ranging from $\delta^{18}O$ = 13.8 to 22.1‰ and $\delta^{13}C$ = -5.22 to 1.12‰ and scattered around a mean value of $\delta^{18}O$ = 19.1‰ and $\delta^{13}C$ = -1,0‰. Ophicalcites from Tos de la Coustette body plot into a distinct field having an extremely low value of $\delta^{18}O$. ii) Ophicalcites from the Eastern Pyrenean bodies display low dispersion (21.3 to 25.1‰) in $\delta^{18}O$ but variable $\delta^{13}C$ values (1.53 to -2.47‰). Among the Eastern Pyrenean ophicalcites, very poor discrimination can be made based on the composition of veins and matrices since both display almost similar values with mean $\delta^{18}O$ of 23.4‰ in the veins and 24.1‰ in the matrices. The O and C isotope compositions of the nine samples containing both veins and matrices are reported in figure 8. One can observe good correlations between the compositions of matrices and veins with the exception of samples

LHZ8 and LHZ64 whose veins are significantly depleted in ^{18}O and slightly enriched in ^{13}C. We note that the pluri-millimetric size of our sampling drilling spots provide bulk estimates of the isotopic compositions of the veins and matrix but do not allow the complex multistage history recorded in some of the veins to be deciphered (i.e. fig. 6G). The isotope composition of the matrices does not correlate with the variable lithology of the clasts (either ultramafic and/or carbonate), nor with the relative amount of clasts. In contrast the isotopic compositions of the marble clasts are highly variable and plot within a larger field than the matrices and veins (Fig. 7). Also, there is no correlation between the isotopic compositions of clasts and the veins or matrices that host them. Actually, these clasts underwent a strong HT/LP metamorphism and may contain abundant silicates (phyllosilicates, amphiboles, scapolite). Closed-system isotopic equilibration between the carbonate and the silicate phases likely introduced variable isotopic alteration of the carbonate phase, depending on the initial amount of detrital silicates in the sedimentary precursor (see for example Valley, 1986; Boulvais et al., 2000). Also, open-system alteration during syn-metamorphic infiltration possibly caused isotopic shifts, which remain difficult to estimate here because we have no more information on the initial geometry of the clast (for example the distance to a lithological discontinuity). The ophicalcites from the Moncaup body display two distinct generations of carbonates with distinct isotopic compositions (fig. 4C and D). Such differences in isotopic compositions are consistent with the occurrence of two types of textures as described in section IV.

VII. Discussion

VII.1. Origin of the various types of ophicalcites

438 Based on the petrographic descriptions on the one hand and on the stable isotope
439 compositions on the other, we are able to distinguish three main categories of ophicalcites
440 associated with the subcontinental mantle bodies of the northern Pyrenees (table 2).

441 The first type of ophicalcites or *hydrothermal type*, as defined in the Tos de la Coustette body
442 results from peridotite carbonation by veins and pervasive substitution of the serpentinite
443 minerals by low $\delta^{18}O$ calcite. The low $\delta^{18}O$ values of calcite indicate that carbonation
444 occurred from rather hot fluids. Comparable $\delta^{18}O$ values have been measured in ophicalcites
445 formed in oceanic and ophiolitic hydrothermal systems (Lavoie & Cousineau 1995; Artemyev
446 & Zaykov 2010). Due to its low $\delta^{18}O$, the first generation of coarse crystalline calcite veins
447 described in the Moncaup peridotite likely corresponds to this type of hydrothermal
448 ophicalcite. The difference in texture types between the Moncaup and the Tos de la Coustette
449 ophicalcites may be explained by the very different rheology and chemical response to fluid
450 circulation of the unserpentinized peridotite at Moncaup compared with the totally
451 serpentinized peridotite of Tos de la Coustette.

452 The second type of ophicalcites or *tectonically-controlled* type is well characterized in the
453 Urdach body. It consists of massive serpentinized peridotites, indifferently lherzolite or
454 harzburgite, crosscut by successive generations of millimetric to centimetric calcite veins with
455 intermediate isotopic compositions. The tectonic control of calcite crystallization is
456 documented by the distribution of veins along preferential planes and their crack-seal
457 geometry. Such calcite crystallizations likely record the arrival of the peridotite close to
458 seafloor environments, directly under the influence of waters with intermediate temperature.
459 Different generations of veins cross-cutting each other with slight variations in isotopic
460 composition may reflect some temperature variations during the successive steps of fracturing
461 / precipitation. In sample URD 1, a first generation of vein with a lower $\delta^{18}O$ values
462 ($\delta^{18}O$=18.6‰) is cut by a later generation with a higher $\delta^{18}O$ value ($\delta^{18}O$=21.1‰). This is

463 consistent with cooling during vein formations, in consequence of progressive exhumation,
464 provided that the isotopic composition of the invading fluid, and then its source, remained
465 constant throughout the history of this sample.

466 The third type of ophicalcites, dominant in the eastern Pyrenees, is *sedimentary ophicalcite*. It
467 consists of a cogenetic association of calcite vein and polymictic breccias. The matrix-
468 supported to clast-supported polymictic breccias are composed of variable proportions of
469 marbles and UM clastic material. Polymictic compositions and typical sedimentary features
470 such as grain-sorting and cross bedding indicate that these ophicalcites have a sedimentary
471 origin (Clerc et al., 2012). Their wide lithological variety, both in UM and metasedimentary
472 material, likely results from sedimentary transport and mixing. By analogy with neptunian
473 veins observed in other extensional settings (Winterer et al. 1991), the micrite-filled brittle
474 fractures have been interpreted as very late, near surface fracturing of the exposed ultramafic
475 basement (Lagabrielle & Auzende 1982; Morgan & Milliken 1996), possibly leading to
476 gravitational instabilities: slumping, slope failure, and landslides as described at ODP site 899
477 by Gibson et al. (1996). The sparite-filled veins and veinlets, either reworked in the breccias,
478 smoothly rooted in the matrix or crosscutting clasts and matrix reveal a multistage deposition
479 history, already implied by the presence of breccias clasts reworked in the breccias (Clerc et
480 al. 2012). Bernoulli & Weissert (1985) describe similar cogenetic and simultaneous sediment
481 infillings and calcitic cement precipitation in Alpine ophicalcites. Such fractures must have
482 allowed the circulation of sedimentary fluids or early diagenetic fluids in domains where
483 restricted dimension hindered the penetration of sedimentary material. The isotopic
484 compositions of matrices and veins (Fig. 8) show a good correlation in both the oxygen and
485 carbon systems, which confirm the idea that both features developed from the same reservoir.
486 Since the relationship is valuable on a rather large range of $\delta^{18}O$ and $\delta^{13}C$, one can infer that

487 the system of vein + matrix development was not connected to an external reservoir which
488 would have produced veins with distinct compositions from the ones of the matrices.

489 Precipitation of acicular aragonite has commonly been correlated with warm water
490 temperatures, high Mg/Ca ratios, high salinity, and high carbonate concentrations, conditions
491 reached in the uppermost levels of serpentine seamounts (Haggerty 1987; Lagabrielle et al.
492 1992). Similar thermal and chemical conditions are associated with fibrous, botryoidal calcite
493 occurrences (Folk 1974; Surour & Arafa 1997), and botryoidal calcite could also represent a
494 replacement texture of acicular radiating aragonite (Ross 1991). More equant and bladed
495 sparry calcite has been correlated with cooler, deeper marine or meteoric settings, typically
496 with low Mg, and carbonate concentrations (Folk 1974; Burton & Walter 1987). Instead,
497 geochemical data (trace element and isotopic signatures) from Iberian margin ophicalcites
498 indicate a seawater imprint at temperatures of 10-20°C, consistent with an early Cretaceous
499 seawater only slightly modified by interaction with serpentinized peridotite basement
500 (Milliken & Morgan 1996). For that reason, Morgan & Milliken (1996) suggested that the
501 temporal evolution in the carbonate phase and morphology, from precipitation of aragonite,
502 followed by fibrous, botryoidal calcite and finally to coarse, bladed sparry calcite may be
503 controlled primarily by fluid flow rates through the vein rather than by variations of the
504 chemical and thermal parameters (fig. 9).

505 The low temperature ophicalcites from the Moncaup body (MP84a, b, c) are peculiar in that
506 they have extremely low $\delta^{13}C$ (< -5.00 ‰), indicative of interaction with organic material.
507 Such carbon isotope compositions are commonly observed in karstic or calcrete precipitations
508 from continental/meteoric waters transiting through soils and vegetation. These peculiar
509 ophicalcites are located immediately below the cataclastic formations staking out the
510 detachment fault between the peridotites and the overlying marbles. Due to the solubility and
511 permeability contrast between these two formations, this interface is prone to concentrating

groundwater. However, we cannot specify if the formations observed are contemporaneous of any very early exhumation of the mantle rocks to subaerial (onland) environments in the Cretaceous or if they result from a later karstification and/or replacement of pre-existing ophicarbonates. Regardless the exact explanation, these values strongly differ from the rest of our dataset by a clear shift toward lower $\delta^{13}C$ values, allowing the distinction to be made between a surface-derived cement precipitated in karstic environments and sedimentary ophicalcites deposited in subaqueous conditions.

VII.2. Environmental conditions for the formation of Central and Eastern Pyrenean ophicalcites

The isotopic compositions of the Pyrenean ophicalcites fall into the same field as other ophicalcites from the literature (fig. 7). Only the three samples from Moncaup MP84a, b, and c are out of this range because of their low carbon composition indicative of interactions with carbon from soils, as discussed above. Ophicalcites from the Alps and Apennine were interpreted as having been formed by interaction with seawater moderately heated to 80 to less than 200°C (Barbieri et al. 1979; Barrett & Friedrichsen 1989; Früh-Green et al. 1990; Schwarzenbach 2011) or by sedimentary fluids later re-equilibrated during Alpine metamorphism (Weissert & Bernoulli 1984; Barbieri et al. 1979).

Samples from the Eastern Pyrenees are clearly recognized as sedimentary ophicalcites by their textures. Consistently, the Eastern Pyrenean ophicalcites have the highest $\delta^{18}O$ values measured in our sample set, a feature which is indicative of low temperatures of precipitation at near surface conditions. However, we notice a major difference in the oxygen isotope composition with ophicalcites from the Iberian margin (Agrinier et al. 1988; Evans & Baltuck 1988; Agrinier et al. 1996; Milliken & Morgan 1996; Plas 1997; Skelton & Valley 2000). Indeed, in the Iberian ophicalcites, which precipitated from low temperature seawater, the

536 $\delta^{18}O$ values of calcite are around 31‰ with $\delta^{13}C$ values varying between -1.7 and 2.2‰.
537 Instead, the Eastern Pyrenean sedimentary ophicalcites analyzed in our study have
538 significantly lower $\delta^{18}O$ values (around 24‰) with carbon isotope compositions ranging from
539 -2.5 to 1.4‰, so that even if the envelope of Pyrenean sedimentary ophicalcites mimic the
540 Iberian margin ones, it is displaced in the $\delta^{13}C$ vs. $\delta^{18}O$ space (grey arrow, fig. 7). At least,
541 three hypotheses can be proposed in order to explain these differences (fig. 10).

542 1. Lowering of the O and C isotope compositions could result from a metamorphic imprint
543 with introduction of externally-derived fluids. Isotopic exchanges between neoformed calcites
544 and the mineral silicates, mainly serpentinite, which form a significant portion of the detrital
545 material associated with the sedimentary ophicalcites, may lower the O isotope composition
546 of the calcite. The breccias and ophicalcites rework clasts of pre-rift material that already bear
547 signs of high-grade recrystallization during the regional HT/LP metamorphism, with the
548 development of scapolite and amphibole. The deposition of the breccias and ophicalcites
549 hence occurs after the peak of metamorphism. But the long-lasting mid-cretaceous thermal
550 anomaly is followed by a lower grade metamorphism that affects the Turonian-Senonian post-
551 rift sediments, with a maximum temperature near 350°C (Ternet et al., 1997; Clerc 2012).
552 This later and lower grade metamorphism may hence have affected the ophicalcites and
553 breccias presented in this study. However, the petrographical effect of metamorphism on
554 these rocks seems rather limited since the matrices show only little recrystallization.
555 Furthermore, we would expect that the oxygen isotope composition would be much more
556 variable depending on the fluid/rock ratio. This is the case for a metamorphic-driven
557 alteration of the isotopic signal as shown from the study of the Alpine ophicalcites (Fig. 7;
558 Weissert & Bernoulli 1984; Früh-Green et al. 1990). Also, one would have expected that the
559 veins show more constant composition instead of displaying delta values that correlate with
560 the values of matrices (Fig. 8).

2. The low O and C compositions may be the result of a hot diagenesis from marine porewater during carbonation. This hypothesis, which implies active circulation of relatively hot fluids in the boundary layer between the ultramafic basement and seawater, is consistent with the high geothermal gradients known to characterize the basins of the North Pyrenean Zone during the Albian-Cenomanian period (Dauteuil & Ricou 1989; Golberg & Leyreloup 1990). The thermal gradients for the Albo-Cenomanian metamorphism can be higher than 100°C/km. In such conditions, we may also consider that unconsolidated sediments still soaked with seawater can be rapidly buried and heated to temperatures as high as 50-80°C. At such temperatures, the calcite precipitated from seawater ($\delta^{18}O = 0‰$) would have a $\delta^{18}O$ value of around 23‰ (considering the isotopic fractionation coefficient of Zheng, 2011), a value that compares well with the data of the Eastern ophicalcites. Thermal gradients as high as 160-180°C/km are known in present days, for instance in the Salton Sea geothermal field (Elders et al., 1972; Muffler & White, 1969). Comparable environments can also be found on the top of mantle exhumed in oceanic domains, where hydrothermal fields develop over areas several square kilometerswide (around $2.5km^2$ at the Rainbow hydrothermal site, German et al., 1996; around $2km^2$ at the Lost City hydrothermal site, Kelley et al., 2001, along the Mid-Atlantic Ridge). In similar settings, in the ophiolites of East Liguria, Spooner and Fyfe (1973) describe temperatures as high as 400°C for shallow depth of circa 300 m below the water/rock interface.

3. As a last hypothesis, it may be that the Eastern Pyrenean sedimentary ophicalcites formed in a low-temperature but endorheic environment, dominated by continental waters and possibly disconnected from the ocean. Indeed, the oxygen composition measured here is about 7‰ lower than the present-day marine Iberian ophicalcites, a difference consistent with the difference between marine and unspecific waters with a continental affinity. Note first that a continental environment is not precluded by the existence of marine fauna, which would

have been observed in sediments associated with ophicalcites. The hypothesis of an endorheic environment dominated by continental waters has to be questioned with respect to the paleogeographic reconstructions of the Pyrenean realm during mid-Cretaceous times. These reconstructions point to the existence of a V-shape opening oceanic domain, narrowing from the Bay of Biscay toward the East where it propagates into the continental crust (Jammes et al. 2009 and references therein). The opening of numerous transtensive basins of limited extension in the central and eastern part of the pre-Pyrenean domain may have been such that these basins were endorheic (Le Pichon et al. 1970; Choukroune & Mattauer 1978), partially disconnected from a marine influence at the time of ophicalcite development. This hypothesis is consistent with the stratigraphy of the Albian sediments deposited in disconnected basins separated by positive reliefs (Debroas, 1976, 1990; Souquet et al., 1985). Some of these reliefs such as the future North Pyrenean massifs and the future Axial Zone were emerged, as shown by the outline of the Cenomanian transgression and by evidence of cooling and sedimentary reworking of crustal material (Filleaudeau et al., 2011). Such short wave-length and high amplitude morphology likely resulted from the flexural response of the lithosphere to the extreme crustal stretching due to the extensional Albian-Cenomanian tectonics along the Pyrenean realm. In such conditions, we may envision that the area where mantle has been exhumed was surrounded by subaerial catchments and, at that time possibly disconnected from the sea. A possible present-day analog is represented by the Salton Sea basin, which is an endorheic continental basin located ahead of the propagating oceanic spreading axis of the Gulf of California. Circulations of continental waters within sediments are also described in more opened environments, for example at the foot of the Aden Gulf margins (Lucazeau et al. 2010).

At this time, it is difficult to select between the three hypotheses even if the last one is the simplest in term of the isotopic composition record. Additional informations like fluid

611 inclusion data is needed to strengthen this hypothesis. It remains clear that, regardless of the
612 exact explanation, sedimentary ophicalcites in the Eastern Pyrenees are distinguishable from
613 those in the Central and in the Western Pyrenees.

614 ## VII.3. Western and Eastern Pyrenean ophicalcites: why are they so different?

615 The three types of ophicalcites identified in this study have to be considered within the frame
616 of the exhumation history of the Pyrenean peridotites presented in section III a and c and as
617 summarized in figure 11. We highlight a clear distinction between the Eastern and Western
618 Pyrenean isotope composition of ophicalcites also evidenced by the different degrees of
619 serpentinization of the mantle that host them, by the temperatures of the metamorphic peak in
620 the surrounding metasediments (Choukroune & Seguret, 1973; Golberg & Leyreloup, 1990;
621 Ravier, 1959; Clerc 2012) and by the typologies of ophicalcites (fig. 11). Following our
622 observations, and in accordance with phase stability of serpentine mineral (Andreani et al.
623 2007), it appears that the variable serpentinization degree of the Pyrenean peridotites can be
624 linked, primarily, to the thermal anomaly accompanying their exhumation. Since carbonation
625 postdated serpentinization, the degree of serpentinization appears as a key factor influencing
626 the development of ophicalcites. Volume increase and rheological softening induced by
627 serpentinization tend to favor the development of numerous fractures, allowing an endogenic
628 precipitation of carbonates as observed in the Western ophicalcites. In contrast, the less
629 serpentinized peridotites exposed in Moncaup and in the Eastern Pyrenees must have had a
630 different behavior during uprising to crustal levels. Their contrasting rheology with the
631 surrounding rocks implies that they were probably still massive and competent until
632 exhumation. This could explain the predominance of superficial ophicalcites found in these
633 localities. The fact that the Eastern Pyrenean peridotites remained preserved from
634 hydrothermal circulation may explain their scarce serpentinization. In addition, such a lack of
635 fluid activity may also be responsible for the preservation of high temperature mineral

assemblage since heat was evacuated by convection. The reason of the limited access of fluids to the exhuming peridotites is not yet understood. We could suggest either i) a blanketing effect of the Mesozoic sedimentary cover that would inhibit water infiltration, or ii) fast exhumation in a continental environment with limited amounts of water available for hydrothermal circulations.

Conclusion

On the basis of close fieldwork, petrographic and geochemical considerations, we present the first comprehensive review of the Pyrenean ophicalcites. Our results, in accordance with published studies on worldwide occurrences of ophicalcites allowed us to distinguish and characterize three main types of ophicalcite (table 2): (i) hydrothermal ophicalcites resulting in low $\delta^{18}O$ calcite (13.8‰) pervasively replacing serpentinite; (ii) intermediate or syn-tectonic ophicalcites developed along with brittle discontinuities in the serpentinized mantle rocks, with intermediate calcite isotope compositions ($\delta^{18}O$ around 20.0‰; $\delta^{13}C$ around -1.06‰); (iii) sedimentary ophicalcites occurring as breccias and neptunian dykes, associated with the circulation of syn-sedimentary fluids. The isotopic compositions for this sedimentary type show the highest $\delta^{18}O$ and $\delta^{13}C$ values of the set, consistent with the cold temperatures of precipitation expected in a sedimentary environment. We note a non-linear distribution of the different ophicalcite type along the Pyrenean range, with dominant endogenic ones in the West and dominant exogenic ones in the East. Such a distribution is clearly linked to a difference in serpentinization degrees likely related to the different exhumation histories and subsequent variable thermal anomalies.

We further investigated the possible origins of the fluid and temperatures at which the calcite may have precipitated in both hydrothermal and sedimentary domains. We present three

660 possible explanations for the relatively low values of the sedimentary ophicalcites: i) a post-
661 sedimentary metamorphic imprint; ii) a hot diagenesis in relation to the high regional thermal
662 gradient; iii) sedimentation in an endorheic basin. This last hypothesis is consistent with the
663 paleogeographic reconstructions of isolated Albo-Cenomanian basins at the tip of a
664 propagating rift. Finally, we highlight a major difference between Eastern and Western
665 ophicalcites, linked primarily to the variable degree of serpentinization. Considering the
666 strong control of serpentinization on the rheology of mantle rocks we propose that the
667 formation of different ophicalcites types is controled by the degree of serpentinization,
668 depending itself on the rate and modalities of exhumation of the subcontinental mantle during
669 extreme crustal stretching.

670

Acknowledgments:

This work was made possible thanks to CNRS, Total, and the Action Marges research group (INSU, Total, IFP, BRGM, IFREMER) through a Ph.D. grant to C. Clerc. We thank G. Früh-green and G. Manatschal for their valuable comments that helped improve the quality of the manuscript. We are grateful to B. Smith for improving the English, to J. -C. Ringenbach and Benoit Ildefonse for fruitful discussions and improvement on the quality of the figures, and to C. Nevado for the high quality thin-sections realized at the Géosciences Montpellier laboratory.

References

Abbate, E., Bortolotti, V., & Passerini, P. (1970). Olistostromes and olistoliths. *Sedimentary Geology*, *4*(3-4), 521-557. doi:10.1016/0037-0738(70)90022-9

Agrinier, P., Cornen, G., & Beslier, M. O. (1996). Mineralogical and oxygen isotopic features of serpentinites recovered from the ocean/continent transition in the Iberia abyssal plain. In R. B. Whitmarsh, D. S. Sawyer, A. Klaus, & D. G. Masson (Éd.), *Proceedings of the Ocean Drilling Program, 149 Scientific Results* (Vol. 149, p. 541-552). Ocean Drilling Program.

Agrinier, P., Mével, C., & Girardeau, J. (1988). Hydrothermal Alteration of the Peridotites Cored at the Ocean/Continent Boundary of the Iberian Margin: Petrologic and Stable Isotope Evidence. In G. Boillot, E. L. Winterer, & et al. (Éd.), *Proceedings of the Ocean Drilling Program, 103 Scientific Results* (Vol. 103, p. 225-234). Ocean Drilling Program. Consulté de http://www-odp.tamu.edu/publications/103_SR/103TOC.HTM

Albarède, F., & Michard-Vitrac, A. (1978a). Datation du métamorphisme des terrains secondaires des Pyrénées par des méthodes Ar-Ar et Rb-Sr. Ses relations avec les péridotites associées. *Bulletin de la société géologique de France*, *XX*(7), 681-688. doi:10.1016/ 0012-821X(78)90157-7

Albarède, F., & Michard-Vitrac, A. (1978b). Age and significance of the North Pyrenean metamorphism. *Earth and Planetary Science Letters*, *40*(3), 327-332. doi:10.1016/0012-821X(78)90157-7

Andreani, M., Mével, C., Boullier, A.-M., & Escartín, J. (2007). Dynamic control on serpentine crystallization in veins: Constraints on hydration processes in oceanic peridotites. *Geochemistry Geophysics Geosystems*, *8*(2). doi:10.1029/2006GC001373

Artemyev, D. A., & Zaykov, V. V. (2010). The types and genesis of ophicalcites in Lower Devonian olistostromes at cobalt-bearing massive sulfide deposits in the West Magnitogorsk paleoisland arc (South Urals). *Russian Geology and Geophysics*, *51*(7), 750-763. doi:10.1016/j.rgg.2010.06.003

Avé-Lallemand, H. G. A. (1967). Structural and petrofabric analysis of an « Alpine type » peridotite: The lherzolite of the French Pyrénées. *Leidse Geol. Meded.*, *42*, 1-57.

Azambre, B., & Rossy, M. (1976). Le magmatisme alcalin d'âge crétacé dans les Pyrénées occidentales; ses relations avec le métamorphisme et la tectonique. *Bulletin de la société Géologique de france*, *7*(18), 1725-1728.

Bailey, E. B., & McCallien, W. J. (1960). Some Aspects of the Steinmann Trinity, Mainly Chemical. *Quarterly Journal of the Geological Society*, *116*(1-4), 365 -395. doi:10.1144/gsjgs.116.1.0365

Barbieri, M., Masi, U., & Tolomeo, L. (1979). Stable isotope evidence for a marine origin of ophicalcites from the north-central Apennines (Italy). *Marine Geology*, *30*(3-4), 193-204. doi:10.1016/0025-3227(79)90015-X

Barrère, P., Bouquet, C., Debroas, E.-J., Pélissonier, H., Peybernès, B., Soulé, J.-C., Souquet, P., et al. (1984). Carte géol. France (1/50 000), feuille Arreau (1072). Orléans.

Barrett, T. J., & Friedrichsen, H. (1989). Stable isotopic composition of atypical ophiolitic rocks from east Liguria, Italy. *Chemical Geology: Isotope Geoscience section*, *80*(1), 71-84. doi:10.1016/0168-9622(89)90049-3

Bernoulli, D., & Weissert, H. (1985). Sedimentary fabrics in Alpine ophicalcites, South Pennine Arosa zone, Switzerland. *Geology*, *13*(11), 755-758. doi:10.1130/0091-7613(1985)13<755:SFIAOS>2.0.CO;2

Bogoch, R. (1987). Classification and genetic models of ophicarbonate rocks. *Ofioliti*, *12*, 23-36.

Bonatti, E., Emiliani, C., Ferrera, G., Honnorez, J., & Rydell, H. (1974). Ultramafic carbonate breccias from the equatorial Mid-Atlantic Ridge. *Marine Geology*, *16*, 83-102.

Bonney, T. G. (1879). Notes on some Ligurian and Tuscan serpentinites. *Geol. Mag.*, *6*(2), 362-371.

Bortolotti, V., & Passerini, P. (1970). Magmatic activity. *Sedimentary Geology*, *4*(3-4), 599-624. doi:10.1016/0037-0738(70)90024-2

Boschi, C., Früh-Green, G., Delacour, A., Karson, J. A., & Kelley, D. S. (2006). Mass transfer and fluid flow during detachment faulting and development of an oceanic core complex, Atlantis Massif (MAR 30°N). *Geochemistry Geophysics Geosystems*, *7*, 39 PP. doi:2006 10.1029/2005GC001074

Boulvais P, Fourcade S, Gruau G, Moine B, Cuney M (1998) Persistance of premetamorphic C and O isotopic signatures in marbles subject to Pan-African granulite-facies metamorphism and U-Th mineralization (Tranomaro, southeast Madagascar) *Chemical Geology*, 150, 247-262.

Boulvais P, de Parseval P, D'Hulst A, Paris P (2006) Carbonate alteration associated with talc-chlorite mineralization in the eastern Pyrenees, with emphasis on the St. Barthelemy Massif. Mineralogy and Petrology, 88, 499-526.

Boulvais, P., Ruffet, G., Cornichet, J., & Mermet, M. (2007). Cretaceous albitization and dequartzification of Hercynian peraluminous granite in the Salvezines Massif (French Pyrénées). *Lithos*, *93*(1-2), 89-106. doi:10.1016/j.lithos.2006.05.001

Brotzu, P., Ferrini, V., Masi, U., Morbidelli, L., & Turi, B. (1973). Contributo alla conoscenza delle « Rocce Verdi » dell'Appennino centrale. Nota III. La composizione isotopica della calcite presente in alcuni affioramenti di oficalciti del F 129 (S. Fiora) e sue implicazioni petrologiche. *Period. Mineral.*, *42*, 591-619.

Brun, J. P., & Beslier, M. O. (1996). Mantle exhumation at passive margins. *Earth and Planetary Science Letters*, *142*(1-2), 161-173. doi:10.1016/0012-821X(96)00080-5

Burton, E. A., & Walter, L. M. (1987). Relative precipitation rates of aragonite and Mg calcite from seawater: Temperature or carbonate ion control? *Geology*, *15*(2), 111-114. doi:10.1130/0091-7613(1987)15<111:RPROAA>2.0.CO;2

Canérot, J., & Delavaux, F. (1986). Tectonic and sedimentation on the north Iberian margin, Chainons Béarnais south Pyrenean zone (Pyrenees basco-béarnaises)–New data about the signification of the lherzolites in the Saraillé area. *Comptes Rendus de l'Académie des Sciences - Series II*, *302*(15), 951-956.

Canérot, J., Peybernès, B., & Ciszak, R. (1978). Présence d'une marge méridionale à l'emplacement des Chaînons Béarnais (Pyrénées basco-béarnaises). *Bulletin de la société Géologique de france*, *7*(20), 673-676.

Casteras, M. (1970). Carte géol. France (1/50 000), feuille Oloron-Sainte-Marie (XV-46). Orléans.

Choukroune, P., et M. Séguret. 1973. « Carte structurale des Pyrénées ». ELF-ERAP.

Choukroune, P., & ECORS Team. (1989). The Ecors Pyrenean deep seismic profile reflection data and the overall structure of an orogenic belt. *Tectonics*, *8*(1), PP. 23-39. doi:198910.1029/TC008i001p00023

Choukroune, P., & Mattauer, M. (1978). Tectonique des plaques et Pyrénées: Sur le fonctionnement de la faille transformante nord-Pyrénéenne; comparaisons avec les modèles actuels. *Bulletin de la société géologique* **de France**, *20*, 689-700.

Clerc, C., Lagabrielle, Y., Neumaier, M., Reynaud, J.-Y., & St Blanquat, M. (2012). Exhumation of subcontinental mantle rocks: evidence from ultramafic-bearing clastic deposits nearby the Lherz peridotite body, French Pyrenees. *Bulletin de la Societe Geologique de France*.

781 Clerc, C., Lagabrielle, Y., Vauchez, A., Lahfid, A., Bousquet, R., Dautria J.-M., Labaume, P.
782 (in prep.).
783 Clerc, C. 2012. « Evolution du domaine Nord-Pyrénéen au Crétacé. Amincissement crustal
784 extreme et thermicité élevée: un analogue pour les marges passives ». PhD Thesis,
785 Paris, France: Université Paris 6. http://tel.archives-ouvertes.fr/tel-00787952
786 Cornelius, H. P. (1912). Petrographische untershungen in den Bergen Zwischen Septiner -
787 und Julierpass. *Diss. N. Jahr. Min.*
788 Cortesogno, L., Galbiati, B., & Principi, G. (1981). Descrizione dettagliata di alcuni
789 caratteristici affioramenti di brecce serpentiniche della Liguria orientale ed
790 interpretazione chiave geodinamica. *Ophioliti*, *6*, 47-76.
791 Costa, S., & Maluski, H. (1988). Use of the 40Ar-39Ar stepwise heating method for dating
792 mylonite zones: An example from the St. Barthélémy massif (Northern Pyrenees,
793 France). *Chemical Geology: Isotope Geoscience section*, *72*(2), 127-144.
794 doi:10.1016/0168-9622(88)90061-9
795 Dauteuil, O., & Ricou, L. E. (1989). Une circulation de fluides de haute température à
796 l'origine du métamorphisme crétacé nord-Pyrénéen. *Geo*, *3*(3), 237-250.
797 Debeaux, M., & Thiébaut, J. (1958). Les affleurements du socle paléozoique entre les massifs
798 de la Barousse et de Milhas. *Bull. Soc. Hist. Nat. Toulouse*, *93*, 522-528.
799 Debroas, E.-J. (1976). Sédimentogenèse et position structurale des flyschs crétacés du versant
800 nord des Pyrénées centrales. *Bull. Bur. Rech. Géol. Min.*, *I*(4), 305-320.
801 Debroas, E.-J. (1990). Le flysch noir albo-cenomanien témoin de la structuration albienne à
802 sénonienne de la Zone nord-pyrénéenne en Bigorre (Hautes-Pyrénées, France).
803 *Bulletin de la société Géologique de france*, *8*(2), 273-285.
804 Debroas, E.-J., Canérot, J., & Billotte, M. (2010). Les brèches d'Urdach, témoins de
805 l'exhumation du manteau pyrénéen dans un escarpement de faille vraconnien-

806 cénomanien inférieur (zone nord-pyrénéenne, Pyrénées-Atlantiques, France). *Géologie*
807 *de la France*, *2*, 53-63.
808 Demange, M., Lia-Aragnouet, F., Pouliguen, M., Perrot, X., & Sauvage, H. (1999). Les
809 syénites du castillet (massif de l'agly, pyrénées orientales, France): une roche
810 exceptionnelle dans les pyrénées. *Comptes Rendus de l'Académie des Sciences -*
811 *Series IIA - Earth and Planetary Science*, *329*(5), 325-330. doi:10.1016/S1251-
812 8050(00)88582-1
813 Demeny, A., Vennemann, T., & Koller, F. (2007). Stable isotope compositions of the
814 Penninic ophiolites of the Köszeg-Rechnitz series. *Central European Geology*, *50*(1),
815 29-46. doi:10.1556/CEuGeol.50.2007.1.3
816 Deramond, J., Souquet, P., Fondecave-Wallez, M.-J., & Specht, M. (1993). Relationships
817 between thrust tectonics and sequence stratigraphy surfaces in foredeeps: model and
818 examples from the Pyrenees (Cretaceous-Eocene, France, Spain). *Geological Society,*
819 *London, Special Publications*, *71*(1), 193-219. doi:10.1144/GSL.SP.1993.071.01.09
820 Dick, H. J. B., Tivey, M. A., & Tucholke, B. E. (2008). Plutonic foundation of a slow-
821 spreading ridge segment: Oceanic core complex at Kane Megamullion, 23°30′N,
822 45°20′W. *Geochemistry Geophysics Geosystems*, *9*, 44 PP. doi:2008
823 10.1029/2007GC001645 [Citation]
824 Dietrich, V., Vuagnat, M., & Bertrand, J. (1974). Alpine metamorphism of mafic rocks.
825 *Schweizerische Mineralogische und petrographische Mitteilungen*, *54*, 291-323.
826 Duée, G., Lagabrielle, Y., Coutelle, A., & Fortané, A. (1984). Les lherzolites associées aux
827 Chaînons Béarnais (Pyrénées Occidentales): Mise à l'affleurement anté-dogger et
828 resédimentation albo-cénomanienne. *Comptes Rendus de l'Académie des Sciences -*
829 *Serie II*, *299*, 1205-1209.
830 Elders, Wilfred A., Robert W. Rex, Paul T. Robinson, Shawn Biehler, et Tsvi Meidav. 1972.

« Crustal Spreading in Southern California The Imperial Valley and the Gulf of California Formed by the Rifting Apart of a Continental Plate ». *Science* 178 (4056) (juin 10): 15-24. doi:10.1126/science.178.4056.15.

Evans, C. A., & Baltuck, M. (1988). Low-Temperature Alteration of Peridotite, Hole 637A. In G. Boillot, E. L. Winterer, & et al. (Éd.), *Proceedings of the Ocean Drilling Program, 103 Scientific Results* (Vol. 103, p. 235-239). Ocean Drilling Program. Consulté de http://www-odp.tamu.edu/publications/103_SR/103TOC.HTM

Fabriès, J., Lorand, J.-P., & Bodinier, J.-L. (1998). Petrogenetic evolution of orogenic lherzolite massifs in the central and western Pyrenees. *Tectonophysics*, *292*(1-2), 145-167. doi:10.1016/S0040-1951(98)00055-9

Fabriès, J., Lorand, J.-P., Bodinier, J.-L., & Dupuy, C. (1991). Evolution of the Upper Mantle beneath the Pyrenees: Evidence from Orogenic Spinel Lherzolite Massifs. *Journal of Petrology*, *Special_Volume*(2), 55-76. doi:10.1093/petrology/Special_Volume.2.55

Filleaudeau, P.-Y., F Mouthereau, et R. Pik. 2011. « Thermo-tectonic evolution of the south-central Pyrenees from rifting to orogeny: insights from detrital zircon U/Pb and (U-Th)He thermochronometry ». *Basin Research* 23. doi:10.1111/j.1365-2117.2011.00535.x.

Folk, R. L. (1974). The natural history of crystalline calcium carbonate: effects of magnesium content and salinity. *J. Sediment. Petrol.*, *44*, 40-53.

Fortane, A., Duee, G., Lagabrielle, Y., & Coutelle, A. (1986). Lherzolites and the western « Chainons bearnais » (French Pyrenees): Structural and paleogeographical pattern. *Tectonophysics*, *129*(1-4), 81-98. doi:10.1016/0040-1951(86)90247-7

Früh-Green, G., Weissert, H., & Bernoulli, D. (1990). A multiple fluid history recorded in Alpine ophiolites. *Journal of the Geological Society*, *147*(6), 959-970. doi: 10.1144/gsjgs.147.6.0959

German, C. R., G. P. Klinkhammer, et M. D. Rudnicki. 1996. « The Rainbow Hydrothermal Plume, 36°15′N, MAR ». *Geophysical Research Letters* 23 (21): 2979-2982. doi:10.1029/96GL02883.

Gianelli, G., & Principi, G. (1977). Northern Apennine ophiolite: an ancient transcurrent fault zone. *Bolletino della Societa Geologica Italiana*, *96*, 53-58.

Gibson, I. L., Milliken, K. L., & Morgan, J. K. (1996). Serpentinite-Breccia Landslide Deposits Generated during Crustal Extension at the Iberia Margin. In R. B. Whitmarsh, D. S. Sawyer, A. Klaus, & D. G. Masson (Éd.), *Proceedings of the Ocean Drilling Program, 149 Scientific Results* (Vol. 149, p. 571-575). Ocean Drilling Program. Consulté de http://www-odp.tamu.edu/publications/149_SR/149TOC.HTM

Golberg, J.-M., & Leyreloup, A. F. (1990). High temperature-low pressure Cretaceous metamorphism related to crustal thinning (Eastern North Pyrenean Zone, France). *Contributions to Mineralogy and Petrology*, *104*(2), 194-207. doi:10.1007/BF00306443

Golberg, J.-M., & Maluski, H. (1988). Données nouvelles et mise au point sur l'âge du métamorphisme pyrénéen. *C. R. Acad. Sci. Paris*, *306*, 429-435.

Golberg, J.-M., H. Maluski, et A.-F. Leyreloup. 1986. « Petrological and age relationship between emplacement of magmatic breccia, alkaline magmatism, and static metamorphism in the North Pyrenean Zone ». *Tectonophysics* 129 (1–4) (octobre 15): 275-290. doi:10.1016/0040-1951(86)90256-8.

876 Gong, Z., Langereis, C. G., & Mullender, T. A. T. (2008). The rotation of Iberia during the
877 Aptian and the opening of the Bay of Biscay. *Earth and Planetary Science Letters*,
878 *273*(1-2), 80-93. doi:16/j.epsl.2008.06.016
879 Haggerty, J. A. (1987). Petrology and geochemistry of Neogene sedimentary rocks from
880 Mariana forearc seamounts. In B. H. Keating, P. Fryer, R. Batiza, & G. W. Boehlert
881 (Éd.), *Seamounts, Islands and Atolls* (Am. Geophys. Union, Geophys. Monogr. Ser.,
882 Vol. 43, p. 175-186).
883 Haggerty, J. A. (1991). Evidence from fluid seeps atop serpentine seamounts in the Mariana
884 forearc: Clues for emplacement of the seamounts and their relationship to forearc
885 tectonics. *Marine Geology*, *102*(1-4), 293-309. doi:10.1016/0025-3227(91)90013-T
886 Henry, P., Azambre, B., Montigny, R., Rossy, M., & Stevenson, R. K. (1998). Late mantle
887 evolution of the Pyrenean sub-continental lithospheric mantle in the light of new
888 40Ar-39Ar and Sm-Nd ages on pyroxenites and peridotites (Pyrenees, France).
889 *Tectonophysics*, *296*(1-2), 103-123. doi:10.1016/S0040-1951(98)00139-5
890 Hervouët, Y., Torné, X., Fortané, A., Duée, G., & Delfaud, J. (1987). Resédimentation
891 chaotique de méta-ophites et de marbres mésozoïques de la vallée du Job (Pyrénées
892 commingeoises): Relations détritisme/métamorphisme en zone nord-Pyrénéenne. *C. R.*
893 *Acad. Sci.*, II, (305), 721-726.
894 Jammes, S., Manatschal, G., Lavier, L. L., & Masini, E. (2009). Tectonosedimentary
895 evolution related to extreme crustal thinning ahead of a propagating ocean: Example
896 of the western Pyrenees. *Tectonics*, *28*(4). doi:10.1029/2008TC002406
897 Kelemen, P. B., Kikawa, E., Miller, D. J., & et al. (Éd.). (2004). *Proceedings of the Ocean*
898 *Drilling Program, 209 Initial Reports* (Vol. 209). Ocean Drilling Program. Consulté
899 de http://www-odp.tamu.edu/publications/209_IR/209TOC.HTM
900 Kelley, Deborah S., Jeffrey A. Karson, Donna K. Blackman, Gretchen L. Früh-Green, David

A. Butterfield, Marvin D. Lilley, Eric J. Olson, et al. 2001. « An Off-axis Hydrothermal Vent Field Near the Mid-Atlantic Ridge at 30° N ». *Nature* 412 (6843) (juillet 12): 145-149. doi:10.1038/35084000.

Knipper, A. L. (1978). Ophicalcites and some other types of breccias accompanying the preorogenic formation of ophiolite complex. *Geotektonika*, *2*, 50-66.

Knipper, A. L., & Sharas'kin, A. Y. (1998). Exhumation of the upper-mantle and lower-crust rocks during rifting. *Geotektonika*, *5*, 19-31.

Lagabrielle, Y., & Auzende, J.-M. (1982). Active in situ disaggregation of oceanic crust and mantle on Gorringe Bank: analogy with ophiolitic massives. *Nature*, *297*(5866), 490-493.

Lagabrielle, Y., Bideau, D., Cannat, M., Karson, J. A., & Mével, C. (1998). Ultramafic-mafic plutonic rock suites exposed along the Mid-Atlantic ridge (10°N-30°N). Symmetrical-asymetrical distribution and implications for seafloor spreading processes. *Faulting and magmatism at mid-ocean ridges*, Geophysical monograph (American Geophysical Union., p. 153-176). Washington, D.C.: Buck W. R., Delaney P. T., Karson J. A., Lagabrielle Y.

Lagabrielle, Y., & Bodinier, J.-L. (2008). Submarine reworking of exhumed subcontinental mantle rocks: field evidence from the Lherz peridotites, French Pyrenees. *Terra Nova*, *20*(1), 11-21. doi:10.1111/j.1365-3121.2007.00781.x

Lagabrielle, Y., & Cannat, M. (1990). Alpine Jurassic ophiolites resemble the modern central Atlantic basement. *Geology*, *18*(4), 319-322. doi:10.1130/0091-7613(1990)018<0319:AJORTM>2.3.CO;2

Lagabrielle, Y., Karpoff, A.-M., & Cotten, J. (1992). Mineralogical and Geochemical Analyses of Sedimentary Serpentinites from Conical Seamount (Hole 788A): Implication for the Evolution of Serpentine Seamounts. In P. Fryer, J. A. Pearce, L. B.

Stokking, & et al. (Éd.), *Proceedings of the Ocean Drilling Program, 125 Scientific Results* (Vol. 125, p. 325-342). Ocean Drilling Program. Consulté de http://www-odp.tamu.edu/publications/125_SR/125TOC.HTM

Lagabrielle, Y., Labaume, P., & St Blanquat, M. (2010). Mantle exhumation, crustal denudation, and gravity tectonics during Cretaceous rifting in the Pyrenean realm (SW Europe): Insights from the geological setting of the lherzolite bodies. *Tectonics*, *29*(4). doi:10.1029/2009TC002588

Lavoie, D., & Cousineau, P. A. (1995). Ordovician ophicalcites of southern Quebec Appalachians; a proposed early seafloor tectonosedimentary and hydrothermal origin. *Journal of Sedimentary Research*, *65*(2a), 337-347. doi:10.1306/D42680B8-2B26-11D7-8648000102C1865D

Laznicka, P. (1988). *Breccias and Coarse Fragmentites: Petrology, Environments, Associations, Ores*. Elsevier Science Ltd.

Le Pichon, X., Bonnin, J., & Sibuet, J.-C. (1970). La faille nord-Pyrénéenne: Faille transformante liée à l'ouverture du Golfe de Gascogne. *Comptes Rendus de l'Académie des Sciences*, D, *271*, 1941-1944.

Lemoine, M. (1980). Serpentinites, gabbros and ophicalcites in the Piemont-Ligurian domain of the Western Alps: Possible indicators of océanic fracture zone and of associated serpentinite protrusions in the Jurassic-Cretaceous Thetys. *Archives des Sciences Genèves*, *33*, 103-115.

Lemoine, M., Tricart, P., & Boillot, G. (1987). Ultramafic and gabbroic ocean floor of the Ligurian Tethys (Alps, Corsica, Apennines): In search of a genetic imodel. *Geology*, *15*(7), 622-625. doi:10.1130/0091-7613(1987)15<622:UAGOFO>2.0.CO;2

Lucazeau, Francis, Sylvie Leroy, Frédérique Rolandone, Elia d' Acremont, Louise Watremez, Alain Bonneville, Bruno Goutorbe, et Doga Düsünur. 2010. « Heat-flow and

hydrothermal circulation at the ocean–continent transition of the eastern gulf of Aden ». *Earth and Planetary Science Letters* 295 (3–4) (juillet 1): 554- 570. doi:10.1016/j.epsl.2010.04.039.

Manatschal, G. (2004). New models for evolution of magma-poor rifted margins based on a review of data and concepts from West Iberia and the Alps. *International Journal of Earth Sciences*, *93*(3), 432-466. doi:10.1007/s00531-004-0394-7

Mattauer, M., & Choukroune, P. (1974). Les lherzolites des Pyrénées sont des extrusions de matériel ancien dans le Mésozoique nord Pyrénées. *paper presented at 2nd Réunion Annuelle des Sciences de la Terre, Soc. Géol. de Fr., Paris*.

McCrea, J. M. (1950). On the isotope chemistry of carbonates and a paleotemperature scale. *J. Chem. Phys.*, *18*, 849-857.

Milliken, K. L., & Morgan, J. K. (1996). Chemical Evidence for Near-Seafloor Precipitation of Cacite in Serpentinites (Site 897) and Serpentinite Breccias (Site 899), Iberia Abyssal Plain. In R. B. Whitmarsh, D. S. Sawyer, A. Klaus, & D. G. Masson (Éd.), *Proceedings of the Ocean Drilling Program, 149 Scientific Results* (Vol. 149, p. 553-558). Ocean Drilling Program. Consulté de http://www-odp.tamu.edu/publications/149_SR/149TOC.HTM

Minnigh, L. D., van Calsteren, P. W. C., & den Tex, E. (1980). Quenching: An additional model for emplacement of the Iherzolite at Lers (French Pyrenees). *Geology*, *8*(1), 18. doi:10.1130/0091-7613(1980)8<18:QAAMFE>2.0.CO;2

Moine, B., Fortune, J. P., Moreau, P., & Viguier, F. (1989). Comparative mineralogy, geochemistry, and conditions of formation of two metasomatic talc and chlorite deposits; Trimouns (Pyrenees, France) and Rabenwald (Eastern Alps, Austria). *Economic Geology*, *84*(5), 1398 -1416. doi:10.2113/gsecongeo.84.5.1398

975 Monchoux, P. (1970). *Les lherzolites pyrénéennes: contribution à l'étude de leur minéralogie,*
976 *de leur génèse et de leurs transformations* (Thèse d'Etat). Univ. Toulouse.
977 Montigny, R., Azambre, B., Rossy, M., & Thuizat, R. (1986). K-Ar Study of cretaceous
978 magmatism and metamorphism in the pyrenees: Age and length of rotation of the
979 Iiberian Peninsula. *Tectonophysics*, *129*(1-4), 257-273. doi:10.1016/0040-
980 1951(86)90255-6
981 Morgan, J. K., & Milliken, K. L. (1996). Petrography of Calcite Veins in Serpentinized
982 Peridotite Basement Rocks from the Iberia Abyssal Plain, Sites 897 and 899:
983 Kinematic and Environmental Implications. In R. B. Whitmarsh, D. S. Sawyer, A.
984 Klaus, & D. G. Masson (Éd.), *Proceedings of the Ocean Drilling Program, 149*
985 *Scientific Results* (Vol. 149, p. 559-569). Ocean Drilling Program. Consulté de
986 http://www-odp.tamu.edu/publications/149_SR/149TOC.HTM
987 Muffler, L. J. Patrick, et Donald E. White. 1969. « Active Metamorphism of Upper Cenozoic
988 Sediments in the Salton Sea Geothermal Field and the Salton Trough, Southeastern
989 California ». *Geological Society of America Bulletin* 80 (2) (janvier 2): 157-182.
990 doi:10.1130/0016-7606(1969)80[157:AMOUCS]2.0.CO;2.
991 Muñoz, J. A. (1992). Evolution of a continental collision belt: ECORS-Pyrenees crustal
992 balanced cross-section. *Thrust Tectonics* (Chapman and Hall., p. 235-246). London:
993 K. McClay.
994 Ohnenstetter, M. (1979). La série ophiolitifère de Rospigliano (Corse) est-elle un témoin des
995 phénomènes tectoniques, sédimentaires et magmatiques liés au fonctionnement des
996 zones transformantes? *Comptes Rendus de l'Académie des Sciences, Paris*, D, *289*,
997 1199-1202.
998 Olivet, J. L. (1996). La cinématique de la plaque ibérique. *Bull. Cent. Rech. Explor. Prod. Elf-*
999 *Aquitaine*, *20*(1), 131-195.

1000 Passchier, C. W. (1984). Mylonite-Dominated Footwall Geometry in a Shear Zone, Central
1001 Pyrenees. *Geological Magazine*, *121*(05), 429-436. doi:10.1017/S0016756800029964
1002 Peters, T. (1965). A water-bearing andradite from the Totalp serpentine (Davos, Switzerland).
1003 *Am*, *50*, 1482-1486.
1004 Picazo, S., Cannat, M., Delacour, A., Escartin, J., Rouméjon, S., & Silantyev, S. (2012).
1005 Deformation associated with the denudation of mantle-derived rocks at the Mid-
1006 Atlantic Ridge 13°-15°N: the role of magmatic injections and hydrothermal alteration.
1007 *Geochemistry Geophysics Geosystems*. doi:10.1029/2012GC004121
1008 Plas, A. (1997). *Petrologic and stable isotope constraints on fluid-rock interaction,*
1009 *serpentinization and alteration of oceanic ultramafic rocks* (PhD Thesis). Swiss
1010 Federal Institute of Technology., Swiss.
1011 Poujol, M., Boulvais, P., & Kosler, J. (2010). Regional-scale Cretaceous albitization in the
1012 Pyrenees: evidence from in situ U-Th-Pb dating of monazite, titanite and zircon.
1013 *Journal of the Geological Society, 167*(4), 751-767. doi:10.1144/0016-76492009-144
1014 Puigdefàbregas, C., & Souquet, P. (1986). Tecto-sedimentary cycles and depositional
1015 sequences of the Mesozoic and Tertiary from the Pyrenees. *Tectonophysics*, *129*(1-4),
1016 173-203. doi:10.1016/0040-1951(86)90251-9
1017 Ravier, J. 1959. « Le métamorphisme des terrains secondaires des Pyrénées ». *Mem. Soc.*
1018 *Geol. Fr.* 86: 1-250.
1019 Ross, D. J. (1991). Botryoidal high magnesium calcite cements from the upperCretaceous of
1020 the Mediterranean region. *J, 61*, 349-353.
1021 Roure, F., & Combes, P.-J. (1998). Contribution of the ECORS seismic data to the Pyrenean
1022 geology : Crustal architecture and geodynamic evolution of the Pyrenees. Consulté
1023 de http://cat.inist.fr/?aModele=afficheN&cpsidt=1874322

Schärer, U., de Parseval, P., Polvé, M., & St Blanquat, M. (1999). Formation of the Trimouns talc-chlorite deposit (Pyrenees) from persistent hydrothermal activity between 112 and 97 Ma. *Terra Nova*, *11*(1), 30-37. doi:10.1046/j.1365-3121.1999.00224.x

Schwarzenbach, E. (2011). *Serpentinization, fluids and life: comparing carbon and sulfur cycles in modern and ancient environments* (PhD Thesis). Swiss Federal Institute of Technology., Zurich.

Skelton, A. D. ., & Valley, J. W. (2000). The relative timing of serpentinisation and mantle exhumation at the ocean-continent transition, Iberia: constraints from oxygen isotopes. *Earth and Planetary Science Letters*, *178*(3-4), 327-338. doi:10.1016/S0012-821X(00)00087-X

Smart, P. L., Palmer, R. J., Whitaker, F., & Wright, V. P. (1987). Neptunian dikes and fissures fills: an overview and account of some modern exemples. In N. P. James & P. W. Choquette (Éd.), *Paleokarst* (Springer-Verlag., p. 149-163). New York.

Souquet, P., Debroas, E.-J., Boirie, J.-M., Pons, P., Fixari, G., Dol, J., Thieuloy, J.-P., et al. (1985). Le groupe du Flysch noir (albo-cénomanien) dans les Pyrénées. *Bull. centres de Rech. Exlpo.-Prod. Elf-Aquitaine, Pau*, *9*(1), 183-252.

Spooner, E. T. C., & Fyfe, W. S. (1973). Sub-sea-floor metamorphism, heat and mass transfer. *Contributions to Mineralogy and Petrology*, *42*(4), 287-304. doi:10.1007/BF00372607

St Blanquat, M. (1993). La faille normale ductile du massif du Saint Barthélémy: Evolution hercynienne des massifs nord-pyrénéens catazonaux considérée du point de vue de leur histoire thermique. *Geodin. Acta*, *6*(1), 59-77.

St Blanquat, M., Brunel, M., & Mattauer, M. (1986). Les zones de cisaillements du massif nord Pyrénéen du Saint-Bartelemy, témoins probables del'extension crustale d'âge crétacé. *C*, *303*, 1339-1344.

St Blanquat, M., Lardeaux, J. M., & Brunel, M. (1990). Petrological arguments for high-temperature extensional deformation in the Pyrenean Variscan crust (Saint Barthélémy Massif, Ariège, France). *Tectonophysics*, *177*(1-3), 245-262. doi:10.1016/0040-1951(90)90284-F

Surour, A. A., & Arafa, E. H. (1997). Ophicarbonates: calichified serpentinites from Gebel Mohagara, Wadi Ghadir area, Eastern Desert, Egypt. *Journal of African Earth Sciences*, *24*(3), 315-324. doi:10.1016/S0899-5362(97)00046-8

Teixell, A. (1998). Crustal structure and orogenic material budget in the west central Pyrenees. *Tectonics*, *17*(3), 395-406. doi:199810.1029/98TC00561

Ternet, Yves, M. Colchen, Elie-Jean Debroas, B. Azambre, F. Debon, J.-L. Bouchez, G. Gleizes, et al. 1997. *Notice explicative, Carte géol. France (1/50 000), feuille Aulus les Bains (1086)*. BRGM éd. Orléans: BRGM.

Thiébaut, J., Debeaux, M., Durand-Wackenheim, C., Souquet, P., Gourinard, Y., Bandet, Y., & Fondecave-Wallez, M.-J. (1988). Métamorphisme et halocinèse crétacés dans les évaporites de Betchat le long du chevauchement frontal Nord-Pyrénéen (Haute-Garonne et Ariège, France). *C. R. Acad. Sci. Paris*, *307*(13), 1535-1540.

Thiébaut, J., Durand-Wackenheim, C., Debeaux, M., & Souquet, P. (1992). Métamorphisme des évaporites triasiques du versant nord des Pyrénées centrales et Occidentales. *Bull. Soc. Hist. Nat. Toulouse*, *128*, 77-84.

Treves, B. E., & Harper, G. D. (1994). Exposure of serpentinites on ocean floor. Sequence of faulting and hydrofracturing in the Northern Apennine ophicalcites. *Ophioliti*, *19*, 435-466.

Treves, B. E., Hickmott, D., & Vaggelli, G. (1995). Texture and microchemical data of oceanic hydrothermal calcite veins, Northern Apennine ophicalcites. *Ophioliti*, *20*(2), 111-122.

1074 Trommsdorff, V., Evan, B. W., & Pfeifer, H. R. (1980). Ophicarbonate rocks: metamorphic
1075 reactions and possible origin. *Archives des Sciences Genève*, *33*, 361-364.
1076 Valley, J.W., 1986. Stable isotope geochemistry of metamorphic rocks. In: Valley, J.W.,
1077 Taylor, H.P., Jr., O'Neil, J.R. Eds.., Stable Isotopes in High Temperature Geological
1078 Processes. *Reviews in Mineralogy*, Vol. 16. Mineral. Soc. Am., 445–489.
1079 Vergés, J., & Garcia-Senz, J. (2001). Mesozoic evolution and Cainozoic inversion of the
1080 Pyrenean rift. *Peri-Tethys Memoir 6: Peri-Tethyan Rift/Wrench Basins and Passive*
1081 *Margins* (Mem. Mus. Natl. Hist. Nat., p. 187-212). Paris: P. A. Ziegler et al. Consulté
1082 de http://www.ija.csic.es/gt/gdl/jverges/PDF/Verges_Garcia_2001.pdf
1083 Vielzeuf, D. (1984). *Relations de phases dans le faciès granulite et implications*
1084 *géodynamiques. L'exemple des granulites des pyrénées.* (Thèse). Clermont-Ferrand.
1085 Vielzeuf, D., & Kornprobst, J. (1984). Crustal splitting and the emplacement of Pyrenean
1086 lherzolites and granulites. *Earth and Planetary Science Letters*, *67*(1), 87-96.
1087 doi:10.1016/0012-821X(84)90041-4
1088 Vissers, R. L. M., Drury M. R., Newman J., & Fliervoet T. F. (1997). « Mylonitic
1089 deformation in upper mantle peridotites of the North Pyrenean Zone (France):
1090 implications for strength and strain localization in the lithosphere ». *Tectonophysics,*
1091 279, 303-325. doi:10.1016/S0040-1951(97)00128-5.
1092 Weissert, H., & Bernoulli, D. (1984). Oxygen isotope composition of calcite in Alpine
1093 ophicarbonates: a hydrothermal or Alpine metamorphic signal□? *Eclogae geol. Helv.*,
1094 *77*(1), 29-43.
1095 Wicks, F. J., & Whittaker, E. J. W. (1977). Serpentine textures and serpentinization. *The*
1096 *Canadian Mineralogist*, *15*(4), 459 -488.

1097 Winterer, E. L., Metzler, C. V., & Sart, M. (1991). Neptunian dykes and associated breccias
1098 (Southern Alps, Italy and Switzerland): role of gravity sliding in open and closed
1099 systems. *Sedimentology*, *38*(3), 381-404. doi:10.1111/j.1365-3091.1991.tb00358.x
1100 Zheng, Y. F. (2011). On the theoretical calculations of oxygen isotope fractionation factors
1101 for carbonate-water systems. *Geochemical Journal*, *45*, 341-354.
1102

Table Caption

Table 1: C (vs. PDB) an O (vs. SMOW) isotopes compositions determined for the carbonate fraction of the veins, matrix and clasts from the Pyrenean ophicalcite.

Table 2: Schematic representation of the different types of ophicalcites analyzed in this study.

Figure Caption

Figure 1. Simplified geological map of the Northern Pyrenean belt with location of the peridotite bodies sampled in this study.

Figure 2. A: Simplified geological map of the Urdach and Tos de la Coustette in the Mail Arrouy and Sarrance *Chaînons Béarnais* with sample sites. B: Simplified geologic map of the Aulus basin presenting the extent of exposure of the peridotite bearing deposits surrounding the *Etang de Lherz* area with the location of the Freychinède, Fontête Rouge, and Berqué samples sites.

Figure 3: Photograph of an ultramafic olistolith in the Aulus basin illustrating the progressive transition from polymictic breccias to massive peridotite penetrated by calcitic veins

Figure 4: Macroscopic aspects of some of the western Pyrenean ophicalcites. A and B: development of calcites veins along tectonic discontinuities in the Urdach peridotite body. C: Mesh texture in highly serpentinized peridotite of Tos de la Coustette. D: Pervasive carbonation and veins in Tos de la Coustette peridotite. Calcite veins (E) and cavities infillings (F) in the Moncaup ultramafic body.

Figure 5: Macroscopic aspects of some of the eastern Pyrenean ophicalcites. A: Bimodal litharenite presenting slumps and syn-sedimentary normal faults from Lherz. B: Grain sorting

in polymictic litharenites from Lherz. C and D: Breccia reworking fresh (orange to green) and serpentinized (dark green to black) peridotites in a calcitic matrix from the Lherz ophicalcites. E: Close association of matrix and veins in a typical ophicalcite from Vicdessos. F: Exposure of an ultramafic body presenting a centimetric orange-brown oxidation ring on the contact between peridotites and carbonates (Ercé-Angladure) G: Metric-sized mesh texture in the Bestiac peridotites. H: Detail of F showing calcite veins cross-cutting the latest serpentinite veins.

Figure 6: Microscopic aspects of the Pyrenean ophicalcites. A: Seal crack calcite vein from Urdach in cathodoluminescence (CL) and redrawn. B: Micrometric veinlets from Urdach. C: Botryoidal calcite in a vein from Urdach, in transmitted light and CL. D: Replacement texture of the ophicalcites from Tos de la Coustette, polarized light. F: Clear sparry calcite in veins from Lherz. G: Close vein/matrix association in transmitted light and CL. H: Dogtooth calcite ghosts in recrystallized veins, in polarized light and Redrawn.

Figure 7: $\delta^{13}C$ vs. d18O diagram showing the isotopic compositions of the Pyrenean ophicaclites (veins, matrices and clasts). Shaded areas represent values from the literature for ophicalcites from the Iberian margin and Galicia bank (Evans & Baltuck 1988; Milliken & Morgan 1996; Plas 1997; Skelton & Valley 2000); the Alps and Apennines (Brotzu et al. 1973; Barbieri et al. 1979; Weissert & Bernoulli 1984; Barrett & Friedrichsen 1989; Demeny et al. 2007) and from other hydrothermal ophicalcites (Lavoie & Cousineau 1995; Artemyev & Zaykov 2010).

1154 Figure 8: Comparison of the C and O isotope compositions of calcitic veins and matrices in
1155 the ophicalcites from Eastern Pyrenees.

1156

1157 Figure 9: Comparison of calcite microtextures in veins and matrices from this study and from
1158 the Iberian margin (Morgan & Milliken, 1996).

1159

1160 Figure 10: Cartoons illustrating the three possible mechanisms responsible the low O
1161 composition of the sedimentary ophicalcites from the Eastern Pyrenees.

1162

1163 Figure 11: Sketches presenting the exhumation history of the Eastern and Western Pyrenean
1164 peridotites in the light of our isotope study. Serpentinization processes are represented by
1165 green colors and the formation of ophicalcites by blue colors.

1166

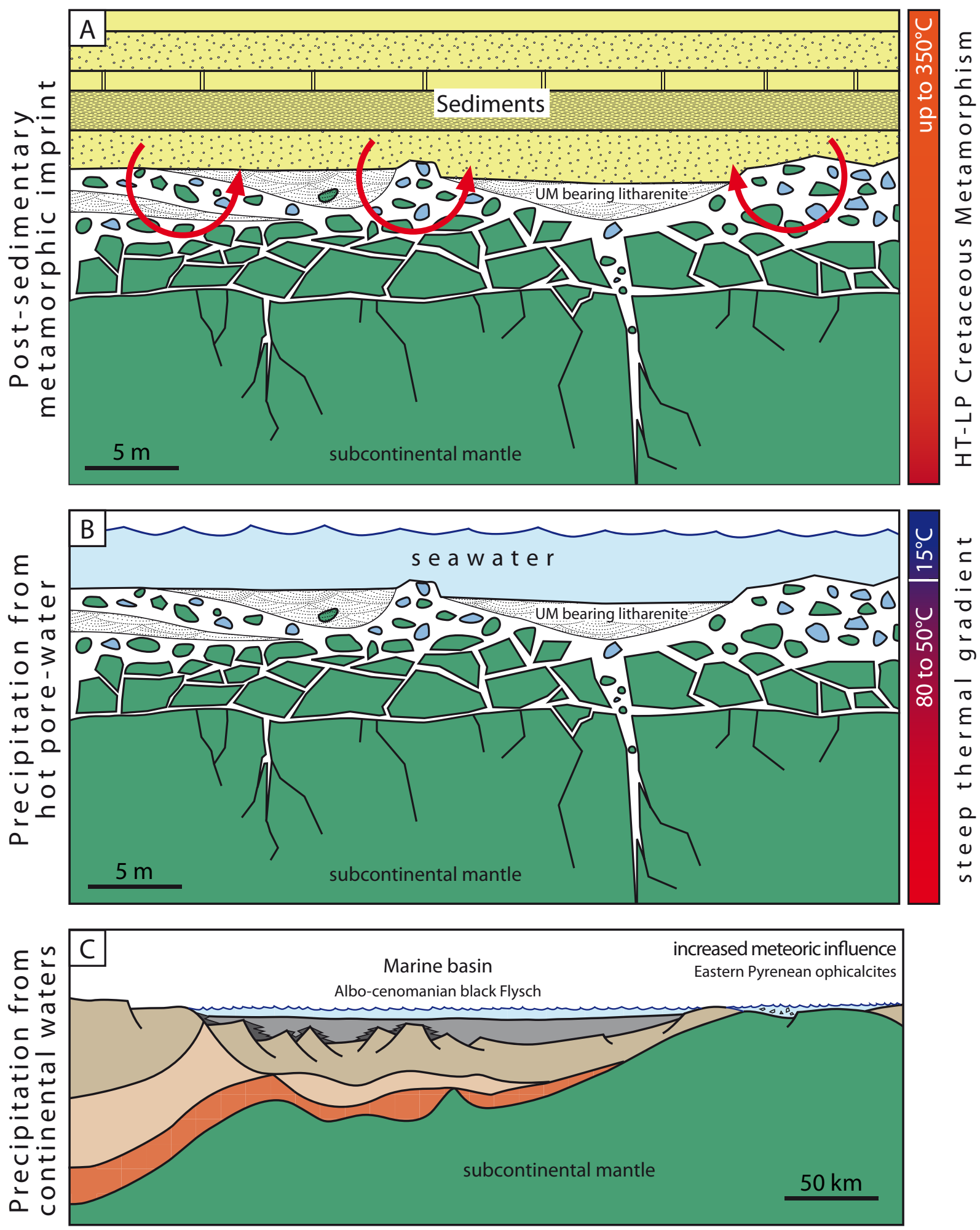
A
Sediments
UM bearing litharenite
5 m
subcontinental mantle
up to 350°C
HT-LP Cretaceous Metamorphism
Post-sedimentary metamorphic imprint
B
seawater
UM bearing litharenite
5 m
subcontinental mantle
15°C
80 to 50°C
steep thermal gradient
Precipitation from hot pore-water
C
Marine basin
Albo-cenomanian black Flysch
increased meteoric influence
Eastern Pyrenean ophicalcites
subcontinental mantle
50 km
Precipitation from continental waters

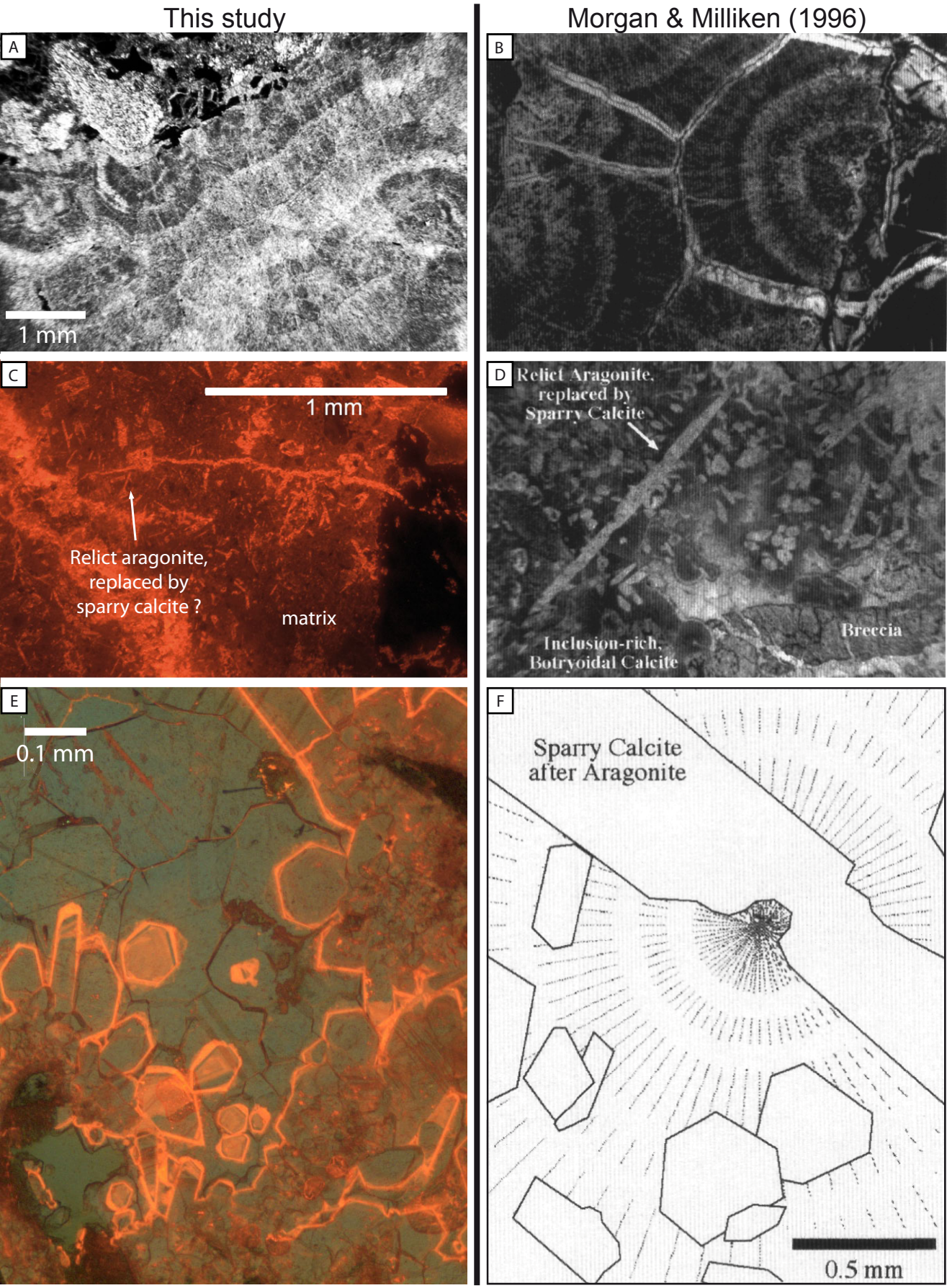

Clerc et al - IJES - Submitted - Figure 9

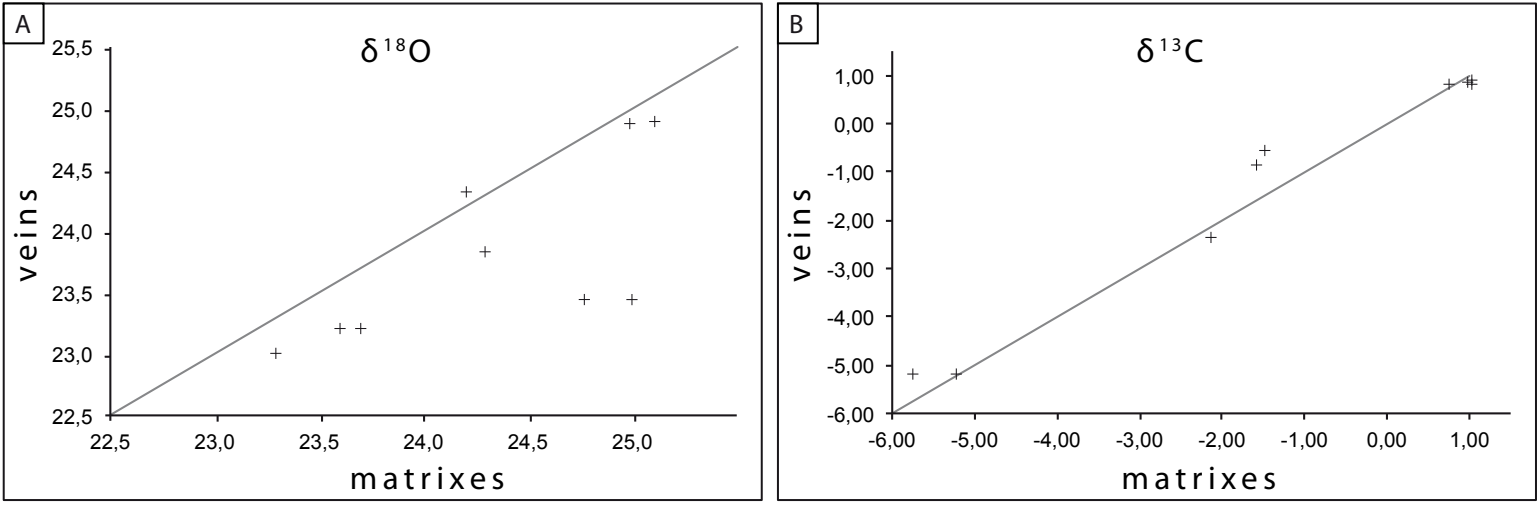

Clerc et al - IJES - Submitted - Figure 8

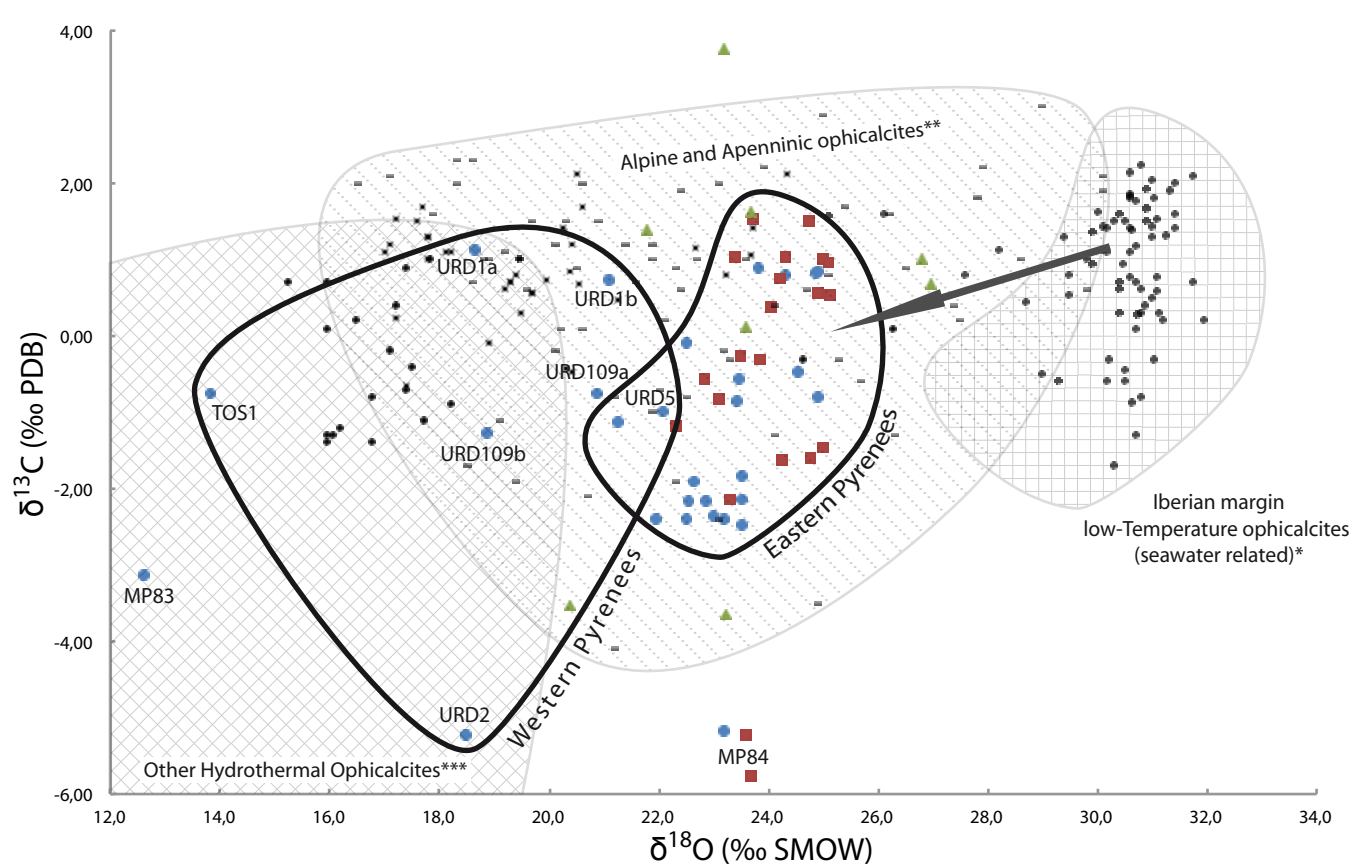

Clerc et al - IJES - Submitted - Figure 7

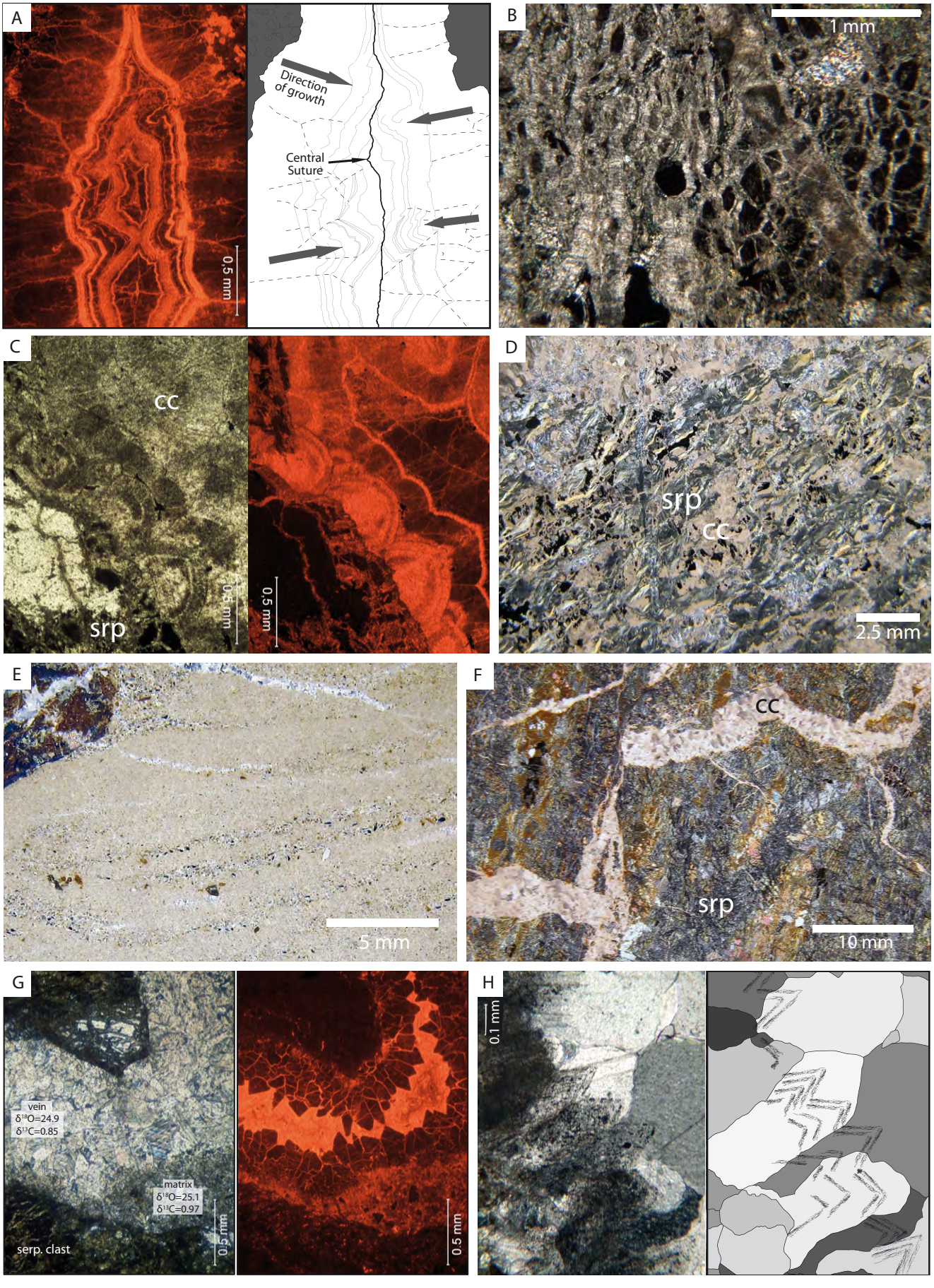

Clerc et al - IJES - Submitted - Figure 6

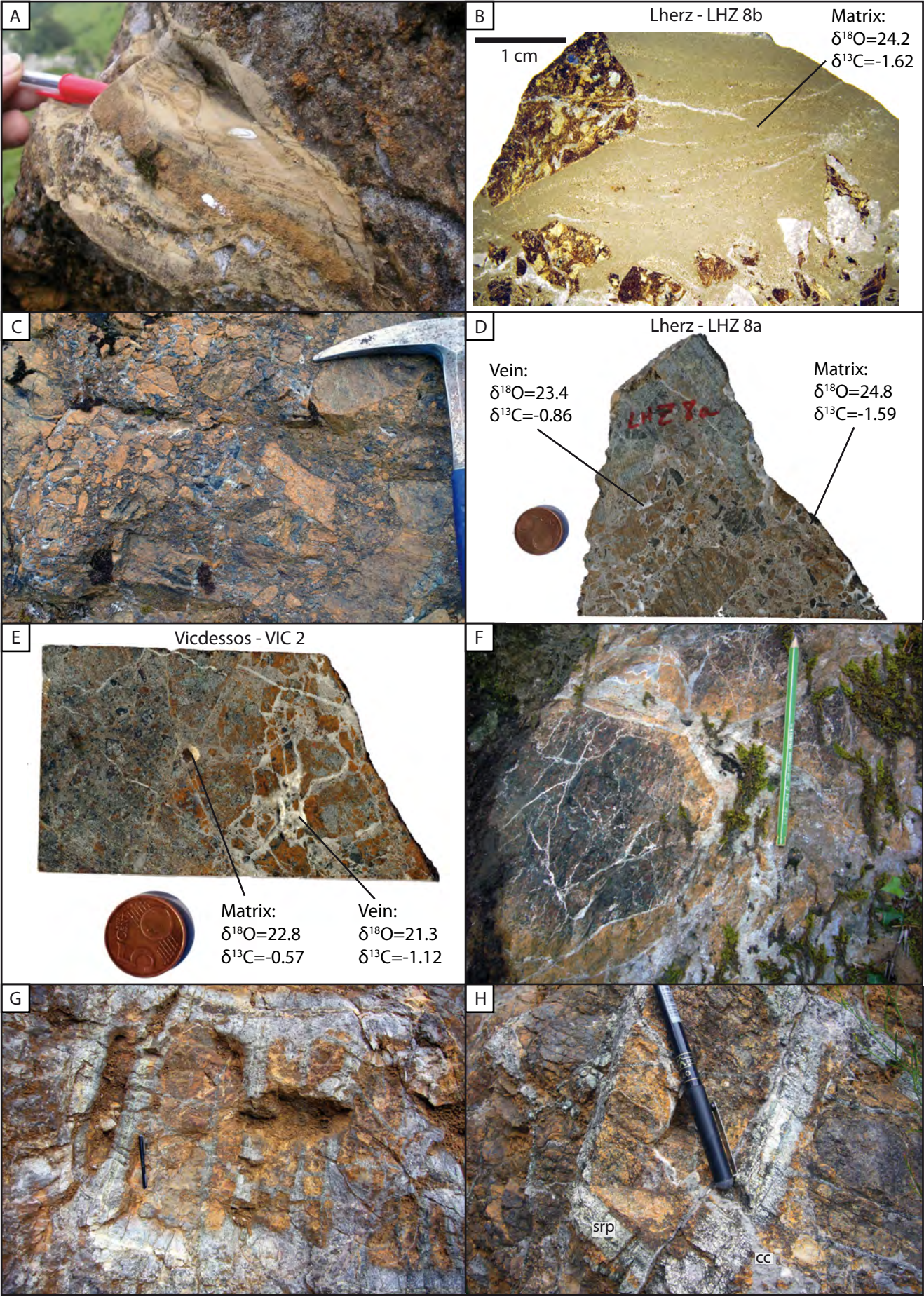

Clerc et al - IJES - Submitted - Figure 5

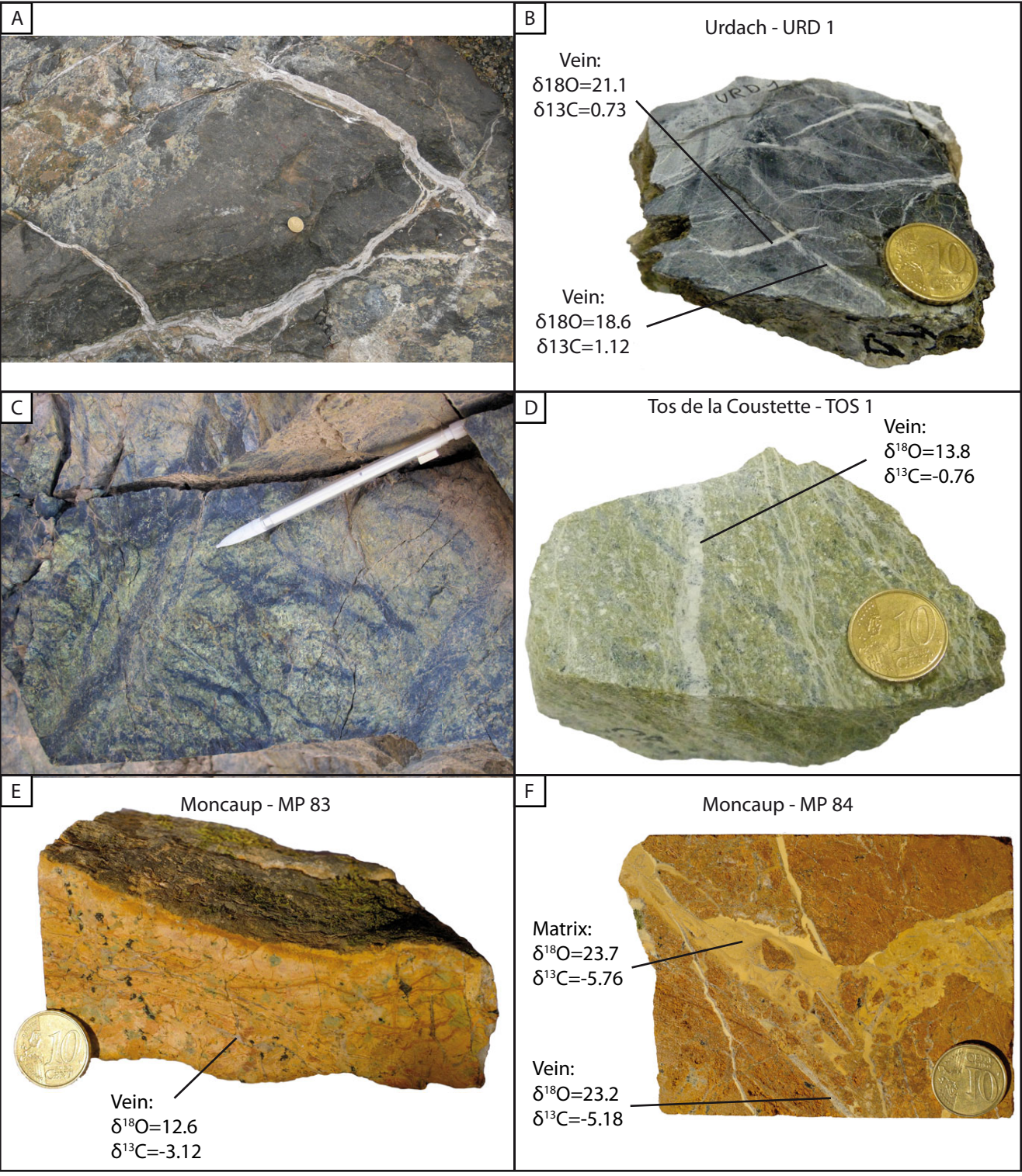

Clerc et al - IJES - Submitted - Figure 4

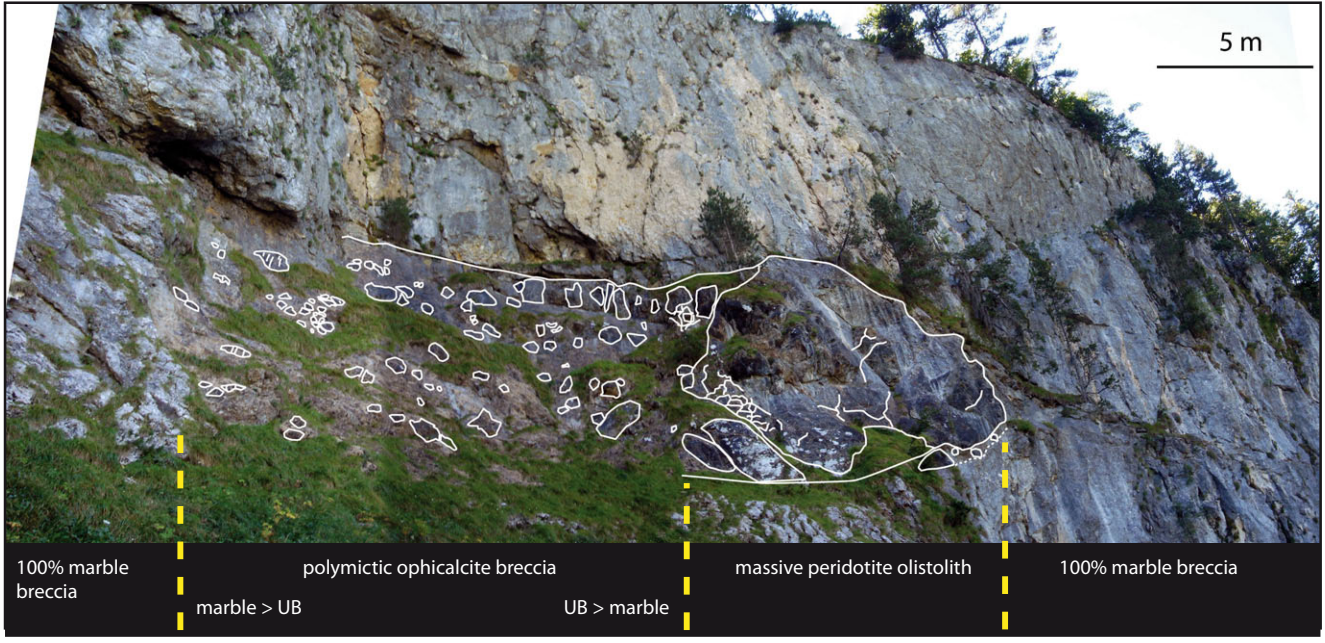

Clerc et al - IJES - Submitted - Figure 3

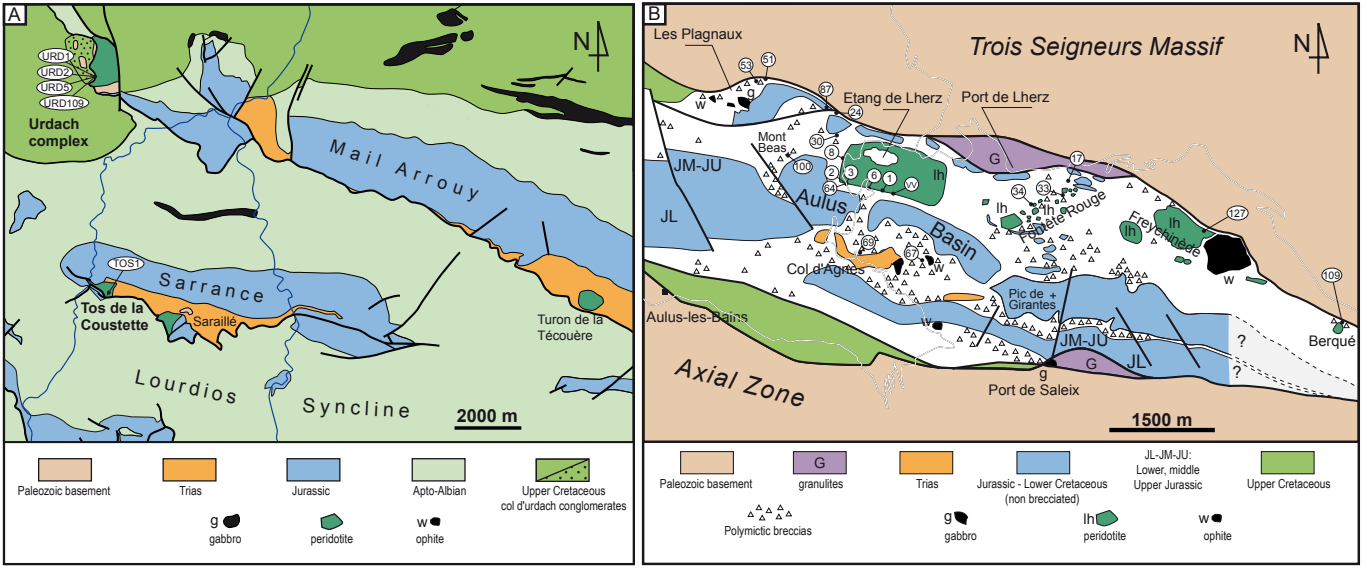

Clerc et al - IJES - Submitted - Figure 2

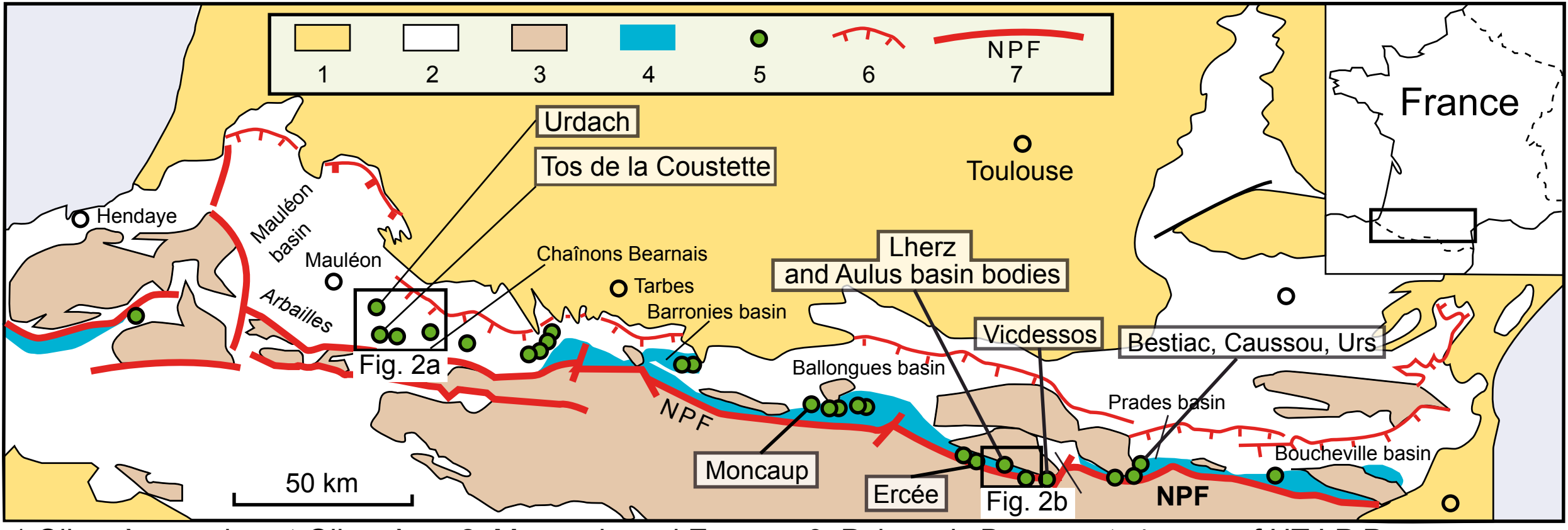

1,Oligocène and post-Oligocène; 2, Mesozoic and Eocene; 3, Paleozoic Basement; 4, area of HT-LP Pyrenean metamorphism; 5, peridotite; 6, main external thrusts; 7, North Pyrenean Fault (NPF)

Clerc et al - IJES - Submitted - Figure 1

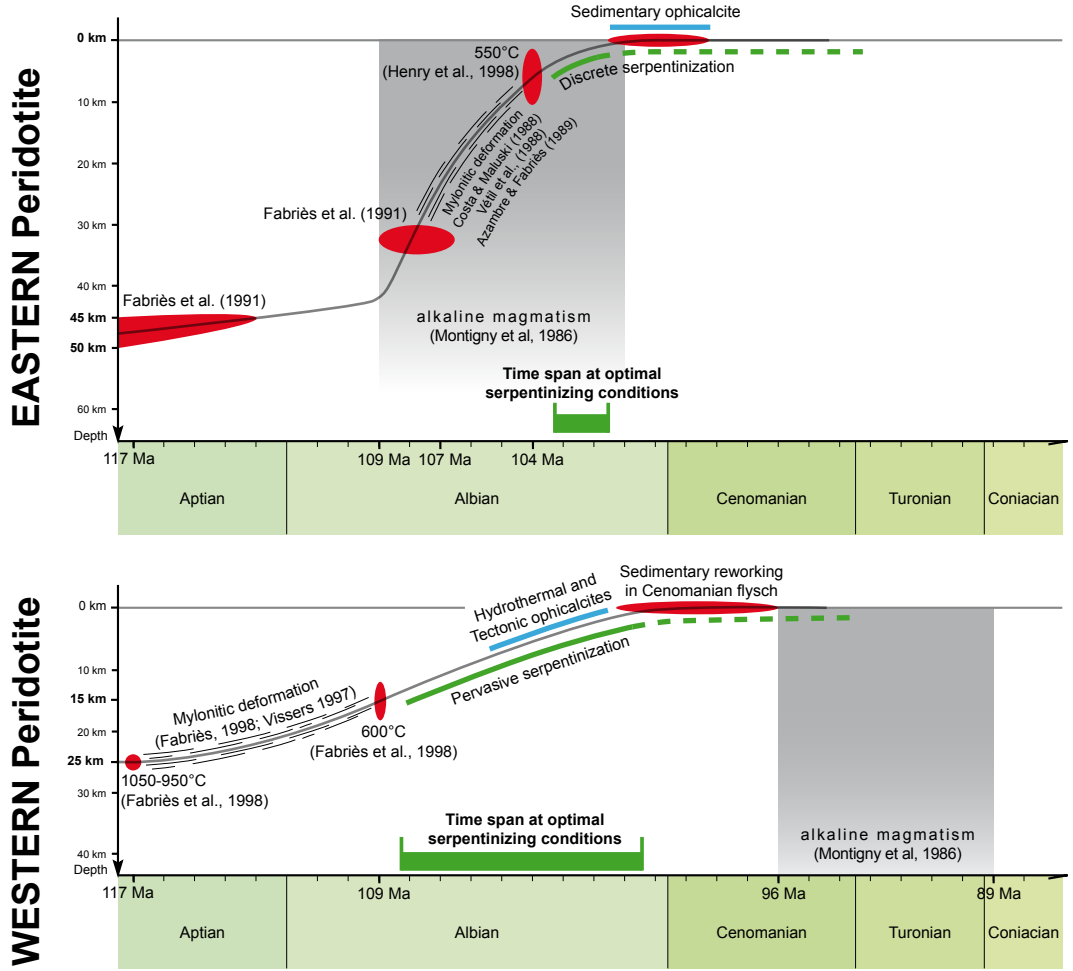

Clerc et al - IJES - Submitted - Figure 11